

Chiral Higgs Mode in Nematic Superconductors

Hiroki Uematsu,¹ Takeshi Mizushima,^{1,*} Atsushi Tsuruta,¹ Satoshi Fujimoto,¹ and J. A. Sauls²

¹Department of Materials Engineering Science, Osaka University, Toyonaka, Osaka 560-8531, Japan

²Center for Applied Physics & Superconducting Technologies

Department of Physics, Northwestern University, Evanston, IL 60208 USA

(Dated: December 26, 2021)

Nematic superconductivity with spontaneously broken rotation symmetry has recently been reported in doped topological insulators, $M_x\text{Bi}_2\text{Se}_3$ ($M=\text{Cu, Sr, Nb}$). Here we show that the electromagnetic (EM) response of these compounds provides a spectroscopy for bosonic excitations that reflect the pairing channel and the broken symmetries of the ground state. Using quasiclassical Keldysh theory, we find two characteristic bosonic modes in nematic superconductors: the nematicity mode and the chiral Higgs mode. The former corresponds to the vibrations of the nematic order parameter associated with broken crystal symmetry, while the latter represents the excitation of chiral Cooper pairs. The chiral Higgs mode softens at a critical doping, signaling a dynamical instability of the nematic state towards a new chiral ground state with broken time reversal and mirror symmetry. Evolution of the bosonic spectrum is directly captured by EM power absorption spectra. We also discuss contributions to the bosonic spectrum from sub-dominant pairing channels to the EM response.

Introduction. Spontaneous symmetry breaking is an important concept that spreads across the diverse fields of modern physics. The recent discovery of two-fold rotation symmetry in superconducting compounds, $M_x\text{Bi}_2\text{Se}_3$ ($M = \text{Cu, Sr, Nb}$), has stimulated an intense discussion of superconductivity with a new class of spontaneous symmetry breaking [1–11]. The rotation symmetry breaking in the basal plane is compatible with odd-parity time-reversal invariant pairing belonging to the two-dimensional irreducible representation (E_u) of the D_{3d} symmetry, which exhibits twofold symmetric gap anisotropy (Fig. 1). The anisotropy is represented by a nematic order parameter [12]. The odd-parity superconductor (SC) $M_x\text{Bi}_2\text{Se}_3$ has also attracted much attention as a prototype of DIII topological SCs that host helical Majorana fermions [13–21]. In addition, there exist competing pairing channels corresponding to the A_{1g} , A_{1u} , and A_{2u} irreducible representations, in addition to the “nematic” E_u state [14].

In this Letter, we report theoretical results showing that the electromagnetic (EM) response at microwave frequencies provides a spectroscopy for long-lived bosonic excitations that are “fingerprints” of the nematic ground state that breaks the maximal symmetry $G = D_{3d} \times T \times U(1)_N$ of the parent compound down to $H = C_{2v} \times T$, where T , $U(1)_N$, and D_{3d} and C_{2v} denote time-reversal symmetry, global gauge symmetry, and point-groups for three- and two-fold rotations, respectively [22]. We first discuss the Fermi-surface evolution that drives the nematic-to-chiral phase transition within the E_u representation. Using the quasiclassical Keldysh theory, we find two characteristic bosonic modes in nematic SCs: the nematicity mode and the chiral Higgs mode. The former corresponding to transverse oscillations of the nematic order parameter is the pseudo-Nambu-Goldstone (NG) boson associated with the broken D_{3d} symmetry. The latter represents the excitation of chiral Cooper pairs. We find that the mass gap of the chiral mode tends to zero as the Fermi surface changes topology from a closed spherical shape to an open cylindrical Fermi surface, signaling the dynamical instability of the nematic state towards the chiral state with broken time-reversal and mirror symmetries. Bosonic modes of unconventional SCs involve the coherent dynamics of macroscopic fractions of electrons, and reflect

the broken symmetries and the sub-dominant pairing interactions [23–37]. The bosonic excitation spectrum can be detected through transverse EM wave absorption [see Fig. 1(a)]. We also consider bosonic modes corresponding to the sub-dominant odd-parity A_{1u} and A_{2u} representations.

Effective Hamiltonian. Electrons embedded in $M_x\text{Bi}_2\text{Se}_3$ exhibit (i) the orbital degrees of freedom, (ii) strong spin-orbit coupling, and (iii) evolution of the Fermi surface with increase in carrier concentration (see Fig. 1) [38, 39]. The low-energy physics is governed by electrons in two p_z -orbitals near the Fermi level. The effective Hamiltonian is given as [40–43]

$$\xi(\mathbf{p}) = c(\mathbf{p}) + m(\mathbf{p})\sigma_x + v_z f_z(p_z)\sigma_y + v(\mathbf{p} \times \mathbf{s})_z \sigma_z - \mu, \quad (1)$$

where $c(\mathbf{p}) = c_0 + c_1 f_\perp(\mathbf{p}) + c_2 p_\parallel^2$, $m(\mathbf{p}) = m_0 + m_1 f_\perp(\mathbf{p}) + m_2 p_\parallel^2$, and μ are the diagonal self-energy correction, band gap, and the chemical potential, respectively ($p_\parallel^2 \equiv p_x^2 + p_y^2$). Nearest-neighbor hopping along the z direction gives $f_z(p_z) = \frac{1}{c} \sin(p_z c)$ and $f_\perp = \frac{2}{c^2} [1 - \cos(p_z c)]$. We take the \hat{z} axis along the (111) direction of the crystal, and \mathbf{s} ($\boldsymbol{\sigma}$) is the spin (orbital) Pauli matrices. The Hamiltonian in Eq. (1) maintains the enlarged D_∞ symmetry including $SO(2)$ about the z -axis, while a higher order correction on p introduces three mirror planes and threefold rotational symmetry in the xy plane [12].

The intercalation of M atoms increases the carrier concentration in the conduction band (CB). As $\mu \gg \Delta$ in typical materials (where Δ is the superconducting gap), low-energy properties of the superconducting states are governed by the CB electrons with the dispersion $E_{CB}(\mathbf{p}) = c - \mu + \sqrt{m^2 + v_z^2 f_z^2 + v^2 p_\parallel^2}$, which is well separated from the valence band by the band gap, $|m_0| \sim \mu$, at the Γ point. Hence, we focus on the Hamiltonian for CB electrons interacting through the odd-parity pairing interaction within $D_{3d} \times T \times U(1)_N$,

$$V_{\mu\nu}(\mathbf{p}, \mathbf{p}') = - \sum_{\Gamma} \sum_{i=1}^{\text{odd}} \sum_{r=1}^{n_r} V_i^{(\Gamma)} d_{\mu,i}^{\Gamma}(\mathbf{p}) d_{\nu,i}^{\Gamma*}(\mathbf{p}'). \quad (2)$$

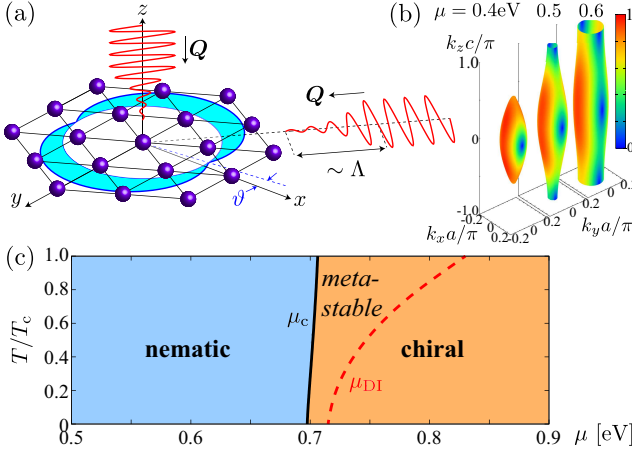


FIG. 1. (a) Configurations of polarized EM waves to probe the nematic pairing gap in the D_{3d} crystal structure. (b) Evolution of the Fermi surface and superconducting gap in the nematic state for various μ . (c) Phase diagram of $M_x\text{Bi}_2\text{Se}_3$ computed by the quasiclassical theory with $\eta_1 = \Delta(T, \mu)$ and $\eta_2 = 0$. We set $T_c^{(E_u, 2)} = T_c$ with $T_c \equiv T_c^{(E_u, 1)}$. The dashed curve shows the dynamical instability of the chiral Higgs mode beyond which the nematic state is no longer metastable.

where $\Gamma = A_{1u}, A_{2u}$, and E_u are the odd-parity irreducible representations of D_{3d} with the dimension n_Γ and basis functions $\{d_1^\Gamma, \dots, d_{n_\Gamma}^\Gamma\}$. The basis functions in lowest order in p are $d_1^{E_u} = (v_z f_z / |m_0|, 0, -vp_x / m_0)$, $d_2^{E_u} = (0, v_z f_z / |m_0|, -vp_y / m_0)$, $d_1^{A_{1u}} = (vp_x / |m_0|, vp_y / |m_0|, v f_z(\mathbf{p}) / m_0)$, and $d_1^{A_{2u}} = (-vp_y, vp_x, 0) / |m_0|$. In the following we utilize the more general form of d_i^Γ [44]. By employing the regularization of gap equations, the pairing interaction of the (Γ, i) channel, $V_i^{(\Gamma)}$, can be related to the instability temperature of the (Γ, i) gap function, $T_c^{(\Gamma, i)}$ [44]. We set $T_c \equiv T_c^{(E_u, 1)}$.

Nematic-to-chiral phase transition. We consider the ground state within the E_u representation, i.e., $T_c \geq T_c^{(E_u, 2)} > T_c^{(A_{1u})}, T_c^{(A_{2u})}$, where the equilibrium odd-parity E_u order parameter in the CB is given by

$$\mathbf{d}(\mathbf{p}) = \eta_1 \mathbf{d}_1^{E_u}(\mathbf{p}) + \eta_2 \mathbf{d}_2^{E_u}(\mathbf{p}). \quad (3)$$

The nematic state with $(\eta_1, \eta_2) = \Delta(\cos \vartheta, \sin \vartheta)$ spontaneously breaks rotational symmetry, and is degenerate with respect to the angle $\vartheta \in [0, \pi/2]$. The broken symmetry is characterized by nematic order, $Q \equiv (|\eta_1|^2 - |\eta_2|^2, \eta_1 \eta_2^* + \eta_1^* \eta_2)$ [12, 45]. The angle ϑ represents the orientation of two point nodes in the xy plane (Fig. 1). Although Eq. (1) respects D_∞ symmetry, corrections to Eq. (1) from hexagonal warping of the Fermi surface pins the nematic angle ϑ to one of three equivalent crystal axes. Another competing order allowed by Eq. (3) is the chiral state with broken time-reversal symmetry, $(\eta_1, \eta_2) = \Delta(1, \pm i)$. The chiral state, $\mathbf{d}_1 \pm i \mathbf{d}_2$, is a non-unitary state with two distinct gaps: one full gap, and another with point nodes at $\mathbf{p} = \pm p_F \hat{z}$.

In Fig. 1(c), we show the phase diagram of $M_x\text{Bi}_2\text{Se}_3$ obtained from quasiclassical theory [44]. The intercalation of M atoms between the quintuple layers modifies the c -axis length of the crystal, namely, the hopping parameters along the z -axis (c_1, m_1, v_z). This makes the Fermi

pocket around the Γ point elongate in the \hat{z} direction. The Fermi surface indeed evolves from a closed spherical shape to a quasi-two-dimensional open cylinder as μ increases [38, 39]. The gap structure of the nematic state changes from a point-nodal to a line-nodal structure as the Fermi surface evolves [Fig. 1(b)] [46]. In contrast, the point nodes of the chiral state disappear and the fully gapped chiral state becomes thermodynamically stable when the Fermi surface is opened in the z -direction. To incorporate the Fermi surface evolution, we follow Ref. [46]: the set of parameters in Ref. [42] for $\mu = 0.4$ eV and the half-value of (c_1, m_1, v_z) for $\mu = 0.65$ eV. The parameters for arbitrary μ are given by interpolating (c_1, m_1, v_z) linearly with respect to μ . With this parametrization, the Fermi surface is opened along the z -axis for $\mu \gtrsim 0.5$ eV. Using this set of parameters, we calculate the thermodynamic potential within the quasiclassical theory, which is valid for $\Delta \ll \mu$. Figure 1 shows the first-order phase boundary between the nematic and chiral ground states near $\mu_c \sim 0.7$ eV. Thus, the nematic-to-chiral phase transition can be driven by Fermi surface evolution, as well as the exchange coupling to magnetic moments of dopant atoms [47, 48] and the thickness of materials [49, 50]. Note that the result obtained above is based on a simple interpolation of the Fermi surface evolution. The phase boundary may be shifted in real materials.

Nematicity and chiral Higgs mode. Consider the nematic state, $\mathbf{d}(\mathbf{p}_F) = \Delta(T, \mu) \mathbf{d}_1^{E_u}(\mathbf{p}_F)$, corresponding to $\vartheta = 0$. The fluctuations in the E_u ground state, $\delta \mathbf{d}(\mathbf{p}_F, \mathbf{Q}, t) \equiv \mathbf{d}(\mathbf{p}_F, \mathbf{Q}, t) - \Delta \mathbf{d}_1^{E_u}(\mathbf{p}_F)$, decompose into the (Γ, j) eigenmodes

$$\delta \mathbf{d}_\mu^C(\mathbf{p}_F, \mathbf{Q}, t) = \sum_{\Gamma} \sum_{j=1}^{n_\Gamma} \mathcal{D}_{\Gamma, j}^C(\mathbf{Q}, t) d_{\mu, j}^\Gamma(\mathbf{p}_F), \quad (4)$$

where \mathbf{Q} is the center-of-mass momentum of Cooper pairs. In the weak-coupling limit, all the bosonic excitations are classified in terms of the parity under particle-hole conversion ($C = \pm$), $\mathcal{D}_j^C = \mathcal{D}_j + C \mathcal{D}_j^*$. The A_{1u} and A_{2u} modes may also exist as long-lived bosons in the spectrum of the nematic state even when $T_c > T_c^{A_{1u}}, T_c^{A_{2u}}$. For $\Gamma = E_u$, there exist four collective modes. Two of these modes are fluctuations in the ground state sector, $\mathcal{D}_{E_u, 1}^C$, the other two modes are in the orthogonal sector $\mathcal{D}_{E_u, 2}^C$. The $\mathcal{D}_{E_u, 1}^C$ modes correspond to the NG mode associated with the broken $U(1)_N$ symmetry ($\mathcal{D}_{E_u, 1}^-$), which is gapped out by the Anderson-Higgs mechanism [51, 52], and $\mathcal{D}_{E_u, 1}^+$ corresponding to the amplitude Higgs mode with mass 2Δ .

The bosonic modes orthogonal to the ground-state sector are represented by $\mathcal{D}_{E_u, 2}^C$. Let us define $\mathcal{D}_{E_u, 2}^+ = \mathcal{D}_{E_u, 2} + \mathcal{D}_{E_u, 2}^* = \Delta \delta \vartheta(t)$ and $\mathcal{D}_{E_u, 2}^- = \mathcal{D}_{E_u, 2} - \mathcal{D}_{E_u, 2}^* = i\epsilon(t)\Delta$, where $\delta \vartheta, \epsilon \in \mathbb{R}$. Thus, $\mathcal{D}_{E_u, 2}^+$ corresponds to $\mathbf{d}(t) = \Delta[\mathbf{d}_1^{E_u} + \delta \vartheta(t) \mathbf{d}_2^{E_u}]$, for $|\delta \vartheta| \ll 1$. This is the pseudo-NG mode associated with the broken rotational symmetry, and represents fluctuations of the nematic order parameter Q . The $\mathcal{D}_{E_u, 2}^-$ mode represents excitation of chiral Cooper pairs, $\mathbf{d}(t) = \Delta[\mathbf{d}_1^{E_u} + i\epsilon(t) \mathbf{d}_2^{E_u}]$. We refer to $\mathcal{D}_{E_u, 2}^+$ and $\mathcal{D}_{E_u, 2}^-$ as the nematicity mode and chiral Higgs mode, respectively.

Let us now consider the linear response to EM fields, $-\frac{e}{c} \mathbf{v}_F \cdot \mathbf{A}(\mathbf{Q}, \omega)$, where \mathbf{A} is a vector potential. The dynam-

ical properties of the superconducting state of $M_x\text{Bi}_2\text{Se}_3$ are governed by Bogoliubov quasiparticles (QPs) in the CB and long-lived bosonic excitations of the pair condensate. The bosonic excitations involve a coherent motion of macroscopic fractions of particles, while low-lying QPs are responsible for the dissipation and the pair-breaking channels. To incorporate the interplay between them, we utilize the quasiclassical Keldysh transport theory [53]. The fundamental quantity is the quasiclassical Keldysh propagator for CB electrons, which contains both Bogoliubov QPs and dynamical bosonic fields, and are governed by the transport-like equation [53–55]. The linear response of the order parameter to the vector potential \mathbf{A} is obtained from the equations of motion

$$\left[\omega^2 - \mathbb{M}_{\Gamma,j}^{\text{C}}(\mathbf{Q}, \omega)\right] \mathcal{D}_{\Gamma,j}^{\text{C}}(\mathbf{Q}, \omega) = \frac{e}{c} Q_{\mu} \zeta_{\mu\nu}^{(\Gamma,j)}(\mathbf{Q}, \omega) A_{\nu}, \quad (5)$$

where $\mathbb{M}_{\Gamma,j}^{\text{C}}$ microscopically determines the mass and lifetime of the mode [44]. Note that particle-hole symmetry prohibits the direct coupling of the $C = +$ nematicity mode to transverse EM fields (i.e., $\zeta = 0$). However, the $C = +$ mode does contribute to the dynamical spin susceptibility [44]. For $C = -$, the coupling of the EM field to the bosonic excitations is governed by the matrix elements

$$\zeta_{\mu\nu}^{(\Gamma,j)}(\mathbf{Q}, \omega) = \Delta \frac{\langle \bar{\lambda}(\mathbf{p}_F, \mathbf{Q}) v_F^{\mu} v_F^{\nu} \mathbf{d}_1^{(E_u)}(\mathbf{p}_F) \cdot \mathbf{d}_j^{(\Gamma)}(\mathbf{p}_F) \rangle_{\text{FS}}}{\langle \bar{\lambda}(\mathbf{p}_F, \mathbf{Q}) | \mathbf{d}_j^{(\Gamma)}(\mathbf{p}_F) \rangle_{\text{FS}}}, \quad (6)$$

where $\langle \dots \rangle_{\text{FS}} \equiv \int dS_p \dots$ is an average over the Fermi surface obtained from Eq. (1) that satisfies $\int dS_p = 1$. The tensor $v_F^{\mu} v_F^{\nu}$ determines the coupling to \mathbf{A} (v_F^{ν}) and \mathbf{Q} (v_F^{μ}), respectively, where $v_F^{\mu} \equiv \partial E_{\text{CM}} / \partial p_{\mu}$ is the Fermi velocity of CB electrons. Hence, $\zeta_{\mu\nu}^{(\Gamma,j)}$ in Eq. (6) determines the coupling of (Γ, j) bosonic modes to EM fields with \mathbf{A} and \mathbf{Q} . The generalized Tsuneto function [56], given by $\bar{\lambda} = \int_{|d|}^{\infty} \frac{d\epsilon}{\sqrt{\epsilon^2 - |d|^2}} \frac{\tanh(\epsilon/2T)}{\epsilon^2 - \omega^2/4}$ for $\mathbf{Q} \rightarrow \mathbf{0}$, is real and positive below the pair-breaking edge $\omega < |d(\mathbf{p}_F)|$, while it has an imaginary part for $\omega > |d(\mathbf{p}_F)|$ which contributes to the dissociation of bosonic modes into Bogoliubov QPs [44, 57].

The dispersion relations, $\omega_{\Gamma,j}^{\text{C}}(\mathbf{Q})$, are determined from Eq. (5) by solving the nonlinear equation, $\omega^2 - \mathbb{M}_{\Gamma,j}^{\text{C}}(\mathbf{0}, \omega) = 0$, which corresponds to a pole of $\delta \mathcal{D}_{\Gamma,j}^{\text{C}} / \delta A_{\mu}$. In Fig. 2, we plot the mass gap of the bosonic modes, $M_{\Gamma,j}^{\text{C}} \equiv \omega_{\Gamma,j}^{\text{C}}(\mathbf{0})$, including the chiral Higgs and nematicity modes. The parameters are the same as those in Fig. 1(c). At $T = 0$, the nematicity mode remains gapless irrespective of μ . The gapless spectrum of the nematicity mode is protected by the enlarged D_{∞} symmetry of Eq. (1), and it is gapped out by terms that are higher-order in p , such as the hexagonal warping energy. Figure 2(b) shows that the mass of the nematicity mode is sensitive to the splitting of T_c of the nematic E_u states.

In Fig. 2, the mass of the chiral Higgs mode decreases as μ increases and softens at the critical value $\mu_{\text{DI}} = 0.71$ at $T = 0$. The softening indicates the dynamical instability of the nematic state towards the chiral state. As shown in Fig. 1(c), the dynamical instability at $T = 0$ takes place in the vicinity of the nematic-to-chiral phase transition μ_c , while it deviates from $\mu_c(T)$ with increasing

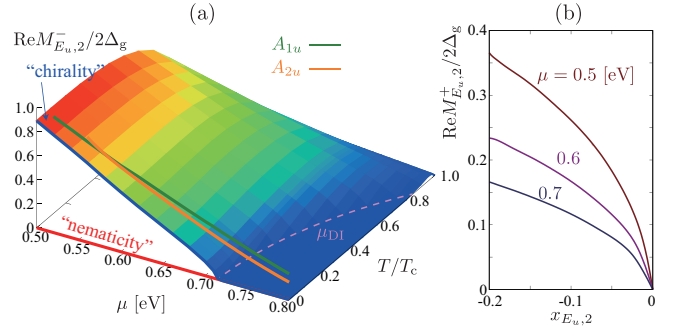


FIG. 2. (a) Mass gap of the chirality mode ($M_{E_u,2}^-$), the nematicity mode ($M_{E_u,2}^+(0, \mu)$), and the A_{1u} and A_{2u} modes as a function of μ . We set $x_{A_{1u}} = x_{A_{2u}} = -1.5$ and $x_{E_u,2} = 0$, where $x_{\Gamma,j} = \ln T_c^{(\Gamma,j)} / T_c$. The color map shows the T -dependence of the chirality mode. The dashed curve corresponds to the dynamical instability of the chirality mode at which the mass gap closes. (b) Mass gap of the nematicity mode as a function of extrinsic symmetry breaking of E_u representation measured by $x_{E_u,2} = \ln(T_c^{(E_u,2)} / T_c)$.

T . This implies that μ_c is the weak first-order transition in low temperatures and the softening can be indeed captured in experiments. The damping of the chirality mode is $-\text{Im} M_{E_u,2}^- / 2\Delta_g = 0.08$ at $\mu = 0.5 \text{ eV}$. The chirality mode has a long lifetime for large μ [see Fig. S3(a) in Ref. [44]]. The QP density of states due to the point nodes decreases as ω^2 , which suppresses the pair-breaking channels for the decay of the chirality mode into QPs residing around the nodal points. Figure 2 also shows that the masses of bosonic modes supported by the competing pairing channels (A_{1u} and A_{2u}) soften and their fluctuations develop as μ increases.

Selection rules and EM absorption spectra. The signatures of the bosonic spectrum and its evolution, inherent to nematic SCs, is reflected in the microwave power absorption spectrum, $P(\omega) = \int d\mathbf{Q} \text{Re}[j(\mathbf{Q}, \omega) \cdot \mathbf{E}^*(\mathbf{Q}, \omega)]$, that is, the Joule losses of the electric field (\mathbf{E}) and current (\mathbf{j}) within the penetration depth $\Lambda = \sqrt{mc^2 / 4\pi ne^2}$ [23, 25–28]. The charge current density is obtained from the quasiclassical propagator as [44]

$$\delta j_{\mu}(\mathbf{Q}) = \sum_{v=x,y,z} \left\{ K_{\mu\nu}^{\text{QP}} - e N_F Q_{\tau} \sum_{\Gamma}^{\text{odd}} \sum_{j=1}^{n_{\Gamma}} \zeta_{\mu\tau,j}^{(\Gamma)} \left(\frac{\delta \mathcal{D}_{\Gamma,j}^{\text{C}}}{\delta A_{\nu}} \right) \right\} A_{\nu}. \quad (7)$$

Equation (7) is the paramagnetic response function, including the vertex corrections from polarization of the medium by bosonic fields [23]. The term, $K_{\mu\nu}^{\text{QP}} = -\frac{2e^2 N_F}{c} \{1 + \frac{(\mathbf{v}_F \cdot \mathbf{Q})^2 (1-\lambda)}{\omega^2 - (\mathbf{v}_F \cdot \mathbf{Q})^2}\} v_F^{\mu} v_F^{\nu} \rangle_{\text{FS}}$, where $\lambda = |d|^2 \bar{\lambda}$, describes the QP contribution to the dissipation via pair-breaking processes. The response, $\delta \mathcal{D}_{\Gamma,j}^{\text{C}} / \delta A_{\nu}$, is obtained from Eq. (5), which has a pole at the collective mode frequency $\omega_{\Gamma,j}^{\text{C}}(\mathbf{Q})$ that satisfies $\omega^2 - \mathbb{M}_{\Gamma,j}^{\text{C}}(\omega) = 0$. For $Q v_F \ll \Delta$ and $v_F / \Lambda \ll \Delta$, the power absorption spectrum is decomposed into the QP contribution and a resonance part from the collective excitations, $P(\omega) = P^{\text{QP}}(\omega) + P^{\text{CM}}(\omega)$ [44].

Equation (6) determines the coupling of bosonic modes of the nematic state with $\mathbf{d} = \Delta \mathbf{d}_1^{(E_u)}$ to the charge current. The ζ function is constrained by symmetries of the

TABLE I. Selection rules for the coupling of transverse EM waves with \mathbf{Q} to the bosonic modes, $\mathcal{D}_{\Gamma,j}^-$ (third-to-sixth columns). The second column denotes the irreducible representations of the ground-state (G.S.) order parameter. We take $\hat{\mathbf{z}}$ along the (111) axis of the D_{3d} crystal.

\mathbf{Q}	G.S.	$\mathcal{D}_{A_{1u}}^-$	$\mathcal{D}_{A_{2u}}^-$	$\mathcal{D}_{E_{u,1}}^-$	$\mathcal{D}_{E_{u,2}}^-$
$\mathbf{Q} \parallel \hat{\mathbf{z}}$	A_{1u}	—	—	—	—
	A_{2u}	—	—	$\mathbf{A} \perp \hat{\mathbf{z}}$	$\mathbf{A} \perp \hat{\mathbf{z}}$
	$E_{u,1}$	—	$\mathbf{A} \perp \hat{\mathbf{z}}$	—	—
	$E_{u,2}$	—	$\mathbf{A} \perp \hat{\mathbf{z}}$	—	—
$\mathbf{Q} \perp \hat{\mathbf{z}}$	A_{1u}	—	—	—	—
	A_{2u}	—	—	$\mathbf{A} \parallel \hat{\mathbf{z}}$	$\mathbf{A} \parallel \hat{\mathbf{z}}$
	$E_{u,1}$	—	$\mathbf{A} \parallel \hat{\mathbf{z}}$	—	$\mathbf{A} \perp \hat{\mathbf{z}}$
	$E_{u,2}$	—	$\mathbf{A} \parallel \hat{\mathbf{z}}$	$\mathbf{A} \perp \hat{\mathbf{z}}$	—

equilibrium order parameter ($d_i^{E_u}$) and bosonic field (d_j^{Γ}). In addition to the chirality mode ($\mathcal{D}_{E_{u,2}}^-$), long-lived massive bosons supported by sub-dominant pairing interactions ($\mathcal{D}_{A_{1u}}^-$ and $\mathcal{D}_{A_{2u}}^-$) are responsible for pronounced absorption peaks in the transverse EM response. In Table I, we summarize the coupling of $\mathcal{D}_{\Gamma,j}^C$ to EM fields with the propagation vectors $\mathbf{Q} \parallel \hat{\mathbf{z}}$ and $\mathbf{Q} \perp \hat{\mathbf{z}}$ for the odd-parity ground-states (A_{1u} , A_{2u} , and E_u). For $\mathbf{Q} = \hat{\mathbf{y}}$ and $\mathbf{A} = \hat{\mathbf{x}}$, the tensor $v_F^\mu v_F^\nu$ in Eq. (6) reduces to $v_F^x v_F^y \sim p_x p_y$. As $\bar{\lambda}$ is an even function on \mathbf{p} , only the chiral Higgs mode with $d_2^{(E_u)}$ couples to the transverse EM field. The selection rules for the ground-states, A_{1u} and A_{2u} , are obtained by replacing $d_1^{E_u}$ to $d^{A_{1u}}$ and $d^{A_{2u}}$ in Eq. (6), respectively. The contributions from the A_{1u} state are prohibited by the enlarged symmetry D_∞ around the small pocket of the Fermi surface. The breaking of $D_\infty \rightarrow D_{3d}$ lifts this super-selection rule. In addition, the coupling of the nematicity mode to the charge current is prohibited by the particle-hole symmetry.

Figure 3 shows the power absorption, $P(\omega)$, and the bosonic excitation contribution, P^{CM} , for the $E_{u,1}$ nematic ground-state at $T = 0.05T_c$ for $\mathbf{Q} \parallel \hat{\mathbf{y}}$ and $\mathbf{A} \parallel \hat{\mathbf{x}}$. According to the selection rules, the EM field couples to only the chiral Higgs mode, $\mathcal{D}_{E_{u,2}}^-$. For $\mu = 0.5\text{eV}$, a broad peak in the spectrum appears around $\omega = 2\Delta_g$. This broad peak arises primarily from the continuum of Bogoliubov QPs, i.e., P^{QP} , and to a lesser extent the chiral Higgs mode, consistent with the large damping rate of the chiral Higgs mode shown in Fig. S3 in Ref. [44]. As μ further increases the broad peak sharpens and shifts to lower frequencies. The pronounced peak originates from resonant absorption of the EM field by the chiral Higgs mode. The shift to lower frequency reflects the softening of the mass gap of these modes. Hence, the precursor to the dynamical instability of the nematic state to the chiral state is captured as a pronounced low-frequency peak in the EM power absorption.

Transverse EM fields with different configurations of $\mathbf{A}(\mathbf{Q})$ couple to different bosonic modes. For instance, the EM field with $\mathbf{A} \parallel \hat{\mathbf{z}}$ and $\mathbf{Q} \parallel \mathbf{x}$ couples to the chiral A_{2u} mode, $d(t) = \Delta d_1^{E_u} + i\epsilon(t)d^{A_{2u}}$. Similarly to Fig. 3, a pronounced low-frequency peak appears in $P(\omega)$ as a consequence of the resonant contribution of the chiral A_{2u} mode (see Fig. S4 in Ref. [44]).

Signature of nematicity mode. Finally, we note that

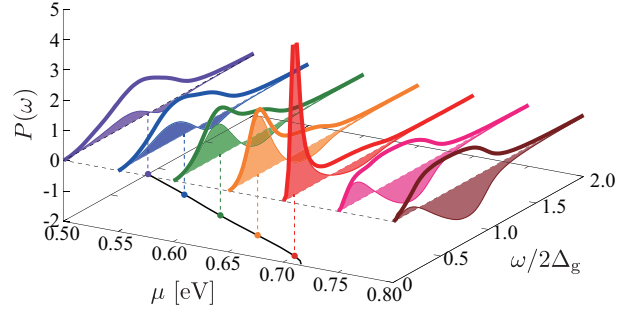


FIG. 3. Power absorption, $P(\omega)$, in the nematic state with the nematic angle $\vartheta = 0$ for $T = 0.05T_c$, where we set $\mathbf{A} \parallel \mathbf{x}$ and $\mathbf{Q} \parallel \mathbf{y}$ and all parameters are same as those in Fig. 2. The shaded area shows the contribution of the bosonic excitations, $P^{\text{CM}}(\omega)$. The mass gaps of the chirality mode, $M_{E_{u,2}}^-$, are also shown.

the nematicity mode makes a significant contribution to dynamical spin susceptibility, $\chi_{zz}(\mathbf{Q}, \omega) = \chi_{zz}^{\text{QP}}(\mathbf{Q}, \omega) + \chi_{zz}^{\text{CM}}(\mathbf{Q}, \omega)$, where $\chi_{zz}^{\text{QP}}(\mathbf{0}, 0)$ is the spin susceptibility of the equilibrium nematic state and χ_{zz}^{CM} corresponds to the response of the nematicity mode (see Sec. S4 in Ref. [44]). As shown in Fig. 2(b), the mass of the nematicity mode is sensitive to $T_c^{(E_{u,2})}/T_c^{(E_{u,1})}$, i.e., weak symmetry-breaking perturbations to the D_∞ . The resulting small mass gap is detected as a pronounced peak in χ_{zz}^{CM} at rf-frequencies resonant with the mass gap. Therefore, dynamical susceptibility measurements may provide a probe for the intrinsic mechanism of pinning the nematic order.

Summary. We have discovered theoretically two characteristic bosonic excitations in nematic SCs: nematicity and chirality modes. The Fermi surface evolution softens the mass gap of the chiral Higgs mode, and the mass shift reflects a distance from the nematic-to-chiral transition in low temperatures. We have also demonstrated that owing to the selection rule, only EM waves with $\mathbf{Q} \perp \mathbf{A} \perp \hat{\mathbf{z}}$ can directly couple to the chiral Higgs mode in nematic SCs. These results show that a pronounced peak observed in absorption measurements can be a direct probe for the chirality excitation energy from the nematic ground state.

Low-lying bosons ubiquitously exist in multi-component SCs with unconventional symmetry breaking, and the selection rule for their EM/magnetic responses is based on the generic argument with the particle-hole symmetry and gap/crystalline symmetries. Hence, EM response provides a spectroscopy of spontaneously broken symmetries and sub-dominant pairing interactions in the broad family of nematic SCs [58–60] and unconventional SCs.

This work was supported by a Grant-in-Aid for Scientific Research on Innovative Areas “Topological Materials Science” (Grants No. JP15H05852, No. JP15H05855, and No. JP15K21717) and “J-Physics” (JP18H04318) and JSPS KAKENHI (Grant No. JP16K05448 and No. JP17K05517). The research of J.A.S. was supported by the National Science Foundation Grant DMR-1508730, and in part by the Aspen Center for Physics, which is supported by National Science Foundation grant PHY-1607611.

Appendix – Supplementary Material

S1. QUASICLASSICAL TRANSPORT THEORY

Here we derive the solutions of the transport equations for the quasiclassical propagator, \check{g} . The propagator is obtained from the Green's function in Keldysh space,

$$\check{G} = \begin{pmatrix} \hat{G}^R & \hat{G}^K \\ 0 & \hat{G}^A \end{pmatrix}, \quad (S1)$$

where \hat{G}^R , \hat{G}^A , and \hat{G}^K are the retarded, advanced, and Keldysh Green's functions in Nambu space, respectively. A key feature of the quasiclassical approximation is that \check{G} is sharply peaked at the Fermi surface embedded in the conduction band, and depends weakly on energies far away from it. We use this assumption to split the propagator into low and high energy parts, $\check{G} = \check{G}^{\text{low}} + \check{G}^{\text{high}}$, where $\check{G}^{\text{low}}(p, Q) = \check{G}(p, Q)$ for $|\varepsilon| < \varepsilon_c$ and otherwise $\check{G}^{\text{low}}(p, Q) = 0$ (p and Q are the relative and center-of-mass momentum, respectively) [61]. The cutoff energy, ε_c , is taken to be $T_c \ll \varepsilon_c \ll E_F$ (T_c is the transition temperature). The high-energy part of this propagator renormalizes bare interactions to effective interactions parametrized by phenomenological parameters, such as effective coupling constant and Landau Fermi liquid parameters. The low-energy propagator defines the quasiclassical Keldysh propagators, \hat{g}^x ($x = R, A, K$) as an integral over a low-energy, long-wavelength shell, $|\mathbf{v}_F \cdot (\mathbf{p} - \mathbf{p}_F)|$, in momentum space near the Fermi surface,

$$\hat{g}^x(\mathbf{p}_F, \varepsilon, Q) = \frac{1}{a} \int_{-\varepsilon_c}^{\varepsilon_c} d\xi_p \hat{\tau}_3 \hat{G}^x(\mathbf{p}, \varepsilon, Q) \\ = \begin{pmatrix} g_0^x + \mathbf{g}^x \cdot \boldsymbol{\sigma} & i\sigma_2 f_0^x + i(\boldsymbol{\sigma} \cdot \mathbf{f}^x)\sigma_2 \\ i\sigma_2 \bar{f}_0^x + i\sigma_2(\boldsymbol{\sigma} \cdot \bar{\mathbf{f}}^x) & \bar{g}_0^x + \bar{\mathbf{g}}^x \cdot \boldsymbol{\sigma}^T \end{pmatrix}, \quad (S2)$$

where $\xi_p = \mathbf{v}_F \cdot (\mathbf{p} - \mathbf{p}_F)$ is the quasiparticle excitation energy, a is the spectral weight of the low-energy quasiparticle resonance and $\boldsymbol{\sigma}^T$ is the transpose of the spin Pauli matrix $\boldsymbol{\sigma}$. We also introduce the abbreviation $Q \equiv (Q, \omega)$. The quasiclassical propagator is governed by Eilenberger's transport equation [54],

$$[i\varepsilon\hat{\tau}_3 - \check{h}(\mathbf{p}_F, Q), \check{g}(\mathbf{p}_F, \varepsilon, Q)]_0 = \eta\check{g}(\mathbf{p}_F, \varepsilon, Q), \quad (S3)$$

where $\eta = \mathbf{v}_F \cdot \mathbf{Q}$. \check{h} is the quasiclassical self-energy matrix in Keldysh space, where $\hat{h}^K = 0$ and $\hat{h}^R = \hat{h}^A \equiv \hat{h}$ is given as

$$\hat{h} = \hat{\Sigma} + \hat{\Delta} = \begin{pmatrix} \Sigma_0 + \boldsymbol{\Sigma} \cdot \boldsymbol{\sigma} & i\sigma_\mu \sigma_2 d_\mu \\ i\sigma_2 \sigma_\mu \bar{d}_\mu & \bar{\Sigma}_0 + \bar{\boldsymbol{\Sigma}} \cdot \boldsymbol{\sigma}^T \end{pmatrix}. \quad (S4)$$

The term, $\hat{\Sigma}$, contains the coupling to an electromagnetic field, and $\hat{\Delta}$ represents the off-diagonal pairing self energy, or order parameter. The transport equation and self energies are supplemented by Eilenberger's normalization condition $\check{g} \circ \check{g} = -\pi^2$ (for the notation, see the main text).

Instead of directly solving the Keldysh transport equation (S3), we derive the Keldysh propagator from the Matsubara propagator by analytic continuation to the real energy axes, e.g. $i\varepsilon_n \rightarrow \varepsilon + i0^+$ followed by $i\omega_m \rightarrow$

$\omega + i0^+$ [55]. Thus,

$$T \sum_{\varepsilon_n} \hat{g}^M(\varepsilon_n; \omega_m) \xrightarrow{i\omega_m \rightarrow \omega + i0^+} \int_{-\varepsilon_c}^{+\varepsilon_c} \frac{d\varepsilon}{4\pi i} \hat{g}^K(\varepsilon; \omega). \quad (S5)$$

To calculate the Keldysh propagator, \hat{g}^K , we generalize the Matsubara transport equation for the two-time/frequency non-equilibrium Matsubara propagator [55],

$$[i\varepsilon\hat{\tau}_3 - \hat{h}] \circ \hat{g}^M - \hat{g}^M \circ [i\varepsilon\hat{\tau}_3 - \hat{h}] - \eta\hat{g}^M = 0 \quad (S6)$$

where the $A \circ B(\varepsilon_{n_1}, \varepsilon_{n_2}) \equiv T \sum_{n_3} A(\varepsilon_{n_1}, \varepsilon_{n_3}) B(\varepsilon_{n_3}, \varepsilon_{n_2})$ is a convolution in Matsubara energies. For the two-frequency propagator, the normalization condition is also a convolution product in Matsubara frequencies,

$$\hat{g}^M \circ \hat{g}^M \equiv T \sum_{\varepsilon_{n_3}} \hat{g}^M(\varepsilon_{n_1}, \varepsilon_{n_3}) \hat{g}^M(\varepsilon_{n_3}, \varepsilon_{n_2}) = -\frac{\pi^2}{T} \delta_{\varepsilon_{n_1}, \varepsilon_{n_2}} \quad (S7)$$

We now express the full propagator as the sum of the equilibrium propagator and a non-equilibrium correction,

$$\hat{g}^M(\mathbf{p}_F, \mathbf{Q}; \varepsilon_{n_1}, \varepsilon_{n_2}) = \hat{g}_0^M(\mathbf{p}_F, \varepsilon_{n_1}) \frac{1}{T} \delta_{\varepsilon_{n_1}, \varepsilon_{n_2}} + \delta\hat{g}^M(\mathbf{p}_F, \mathbf{Q}; \varepsilon_{n_1}, \varepsilon_{n_2}). \quad (S8)$$

Model Hamiltonian and basis functions

The parent materials of carrier-doped topological insulators, $M_x\text{Bi}_2\text{Se}_3$ ($M = \text{Cu, Sr, Nb}$), are composed of spin-1/2 fermions with orbital degrees of freedom. The low-energy structure is governed by two p_z orbitals localized on the lower and upper sides of the quintuple layer. The 4×4 effective Hamiltonian, $\xi(\mathbf{p})$, relevant to the parent material is given by

$$\xi(\mathbf{p}) = c(\mathbf{p}) + m(\mathbf{p})\sigma_x + v_z f(p_z)\sigma_y + v(\mathbf{p} \times \mathbf{s})_z \sigma_z, \quad (S9)$$

where $c(\mathbf{p}) = c_0 + c_1 f_\perp(\mathbf{p}) + c_2 p_\parallel^2$, $m(\mathbf{p}) = m_0 + m_1 f_\perp(\mathbf{p}) + m_2 p_\parallel^2$, and μ are the diagonal self-energy correction, band gap, and the chemical potential, respectively ($p_\parallel^2 \equiv p_x^2 + p_y^2$). Nearest-neighbor hopping along the z direction gives $f_z(p_z) = \frac{1}{c} \sin(p_z c)$ and $f_\perp = \frac{2}{c^2} [1 - \cos(p_z c)]$. We have also introduced the spin and orbital Pauli matrices, s_μ and σ_μ ($\mu = x, y, z$). We take z -axis along the (111) direction of the crystal along which the quintuple layers are stacked by van der Waals gap. The effective Hamiltonian approximately holds the D_∞ including the $\text{SO}(2)_{J_z}$ symmetry about the z -axis, while the higher order correction on p introduces the three mirror planes and threefold rotational symmetry in the xy plane.

In this work, we consider the linear response of nematic superconductors to electromagnetic fields. The vector potential \mathbf{A} is introduced in Eq. (S9) by Peierls substitution, $\mathbf{p} \rightarrow \mathbf{p} - e\mathbf{A}$. In addition, the Zeeman term in the parent topological insulator is given by adding the following term in Eq. (S9)

$$\mathcal{H}_Z = \sum_{\mu, i} \frac{1}{2} g_{i\mu} \mu_B s_i H_i \sigma_\mu, \quad (S10)$$

where μ_B is the Bohr magneton and H_i is the i th component of the Zeeman field ($i = x, y, z$). The g -factor of the parent

topological insulator is given by $g_{i\mu}$ ($\mu = 0, x, y, z$). For Bi_2Se_3 , $g_{x0} = g_{y0} = -8.92$, $g_{z0} = -21.3$, $g_{xx} = g_{yy} = 0.68$, and $g_{zx} = -29.5$ and $g_{i\mu} = 0$ otherwise [41, 42].

Let us now introduce the gap functions belonging to the irreducible representations of the D_{3d} crystalline symmetry of the compounds $M_x\text{Bi}_2\text{Se}_3$. The 4×4 matrix form of the superconducting gap function is given by

$$\Delta(\mathbf{R}) = \sum_{j=1}^{n_\Gamma} \eta_j^{(\Gamma)}(\mathbf{R}) W_j^{(\Gamma)} i s_y, \quad (\text{S11})$$

where $\Gamma = A_{1g}, A_{1u}, A_{2u}, E_u$ are the even-parity and odd-parity irreducible representations of D_{3d} with the dimension n_Γ and the basis functions $\{W_1^{(\Gamma)}, \dots, W_{n_\Gamma}^{(\Gamma)}\}$. The 4×4 matrix $W_j^{(\Gamma)}$ is given as $W_1^{(A_{1g})} = \{1, \sigma_x\}$ for the even parity state, and $W^{(A_{1u})} = \sigma_y s_z$, $W^{(A_{2u})} = \sigma_z$, and $(W_1^{(E_u)}, W_2^{(E_u)}) = (\sigma_y s_x, \sigma_y s_y)$ for the odd-parity states.

The Hamiltonian in Eq. (S9) is diagonalized as $U^\dagger(\mathbf{p}) \xi(\mathbf{p}) U(\mathbf{p}) = \text{diag}[E_{\text{CB}}(\mathbf{p}), E_{\text{VB}}(\mathbf{p})]$. The conduction band energy, $E_{\text{CB}}(\mathbf{p}) = c - \mu + \sqrt{m^2 + v^z f^2 + v^2 p_\parallel^2}$, is separated from the valence band, $E_{\text{VB}}(\mathbf{p}) = c - \mu - \sqrt{m^2 + v^z f^2 + v^2 p_\parallel^2}$, by the band gap $2|m_0|$ at the Γ point. The intercalation of Cu, Sr, and Nb atoms into the van der Waals gap increases the carrier density of the conduction band and generates a small electron Fermi pocket around the Γ point. Since the band gap is $m_0 = -0.28$ eV and μ is the same order as $|m_0|$, both energy scales are much larger than the superconducting gap. Hence, it is natural to employ the quasiclassical approximation which takes account of only the electron states in the conduction band.

Let \mathcal{P}_{CB} be a projection operator onto the conduction band. The pair potential projected onto the conduction band is parameterized with the even-parity scalar field $\psi(\mathbf{p}) = \psi(-\mathbf{p})$ and odd-parity \mathbf{d} -vector field $\mathbf{d}(\mathbf{p}) = -\mathbf{d}(-\mathbf{p})$ as

$$\mathcal{P}_{\text{CB}}[U^\dagger(\mathbf{p}) \Delta U(\mathbf{p})] = \psi(\mathbf{p}) i s_y + i s_\mu s_y d_\mu(\mathbf{p}). \quad (\text{S12})$$

The repeated Greek indices imply the sum over the vector components of the spin $S = 1$ basis, x, y, z , constructed to provide bases of the irreducible representation Γ . $V_i^{(\Gamma)} > 0$ is the coupling constant for the representation Γ . In the band representation [42], the E_u state has $\psi_{1,2}^{(E_u)} = 0$ and

$$\mathbf{d}_1^{(E_u)} = \left[\left(1 - \mathcal{E} \frac{p_y^2}{p_\parallel^2} \right) \frac{v_z p_z}{\tilde{\epsilon}(p_z)}, \mathcal{E} \frac{p_x p_y}{p_\parallel^2} \frac{v_z p_z}{\tilde{\epsilon}(p_z)}, -\frac{m}{\tilde{\epsilon}} \frac{v k_x}{\tilde{\epsilon}(p_z)} \right], \quad (\text{S13})$$

$$\mathbf{d}_2^{(E_u)} = \left[\mathcal{E} \frac{p_x p_y}{p_\parallel^2} \frac{v_z p_z}{\tilde{\epsilon}(p_z)}, \left(1 - \mathcal{E} \frac{p_x^2}{p_\parallel^2} \right) \frac{v_z p_z}{\tilde{\epsilon}(p_z)}, -\frac{m}{\tilde{\epsilon}} \frac{v k_y}{\tilde{\epsilon}(p_z)} \right], \quad (\text{S14})$$

where we set $\tilde{\epsilon} \equiv \sqrt{m^2 + v^z f^2 + v^2 p_\parallel^2}$, $\tilde{\epsilon}(p_z) \equiv \tilde{\epsilon}(0, 0, p_z)$, and $\mathcal{E} \equiv 1 - \tilde{\epsilon}(p_z)/\tilde{\epsilon}(\mathbf{p})$. In the same manner, the basis functions in the band representation are given by

$$\psi_1^{(A_{1g})}(\mathbf{p}) = \{1, m(\mathbf{p})/\tilde{\epsilon}(\mathbf{p})\}, \quad (\text{S15})$$

and $\mathbf{d}_1^{(A_{1g})}(\mathbf{p}) = \mathbf{0}$ for A_{1g} ,

$$\mathbf{d}_1^{(A_{1u})}(\mathbf{p}) = \frac{1}{\tilde{\epsilon}(p_z)} \left(\frac{m(\mathbf{p})}{\tilde{\epsilon}(\mathbf{p})} v p_x, \frac{m(\mathbf{p})}{\tilde{\epsilon}(\mathbf{p})} v p_y, v p_z \right), \quad (\text{S16})$$

and $\psi_1^{(A_{1u})}(\mathbf{p}) = 0$ for A_{1u} , and

$$\mathbf{d}_1^{(A_{2u})}(\mathbf{p}) = (-v p_y, v p_x, 0)/\tilde{\epsilon}(\mathbf{p}), \quad (\text{S17})$$

and $\psi_1^{(A_{2u})}(\mathbf{p}) = 0$ for A_{2u} .

Nematic-to-chiral phase transition: Ginzburg-Landau theory

Using the Ginzburg-Landau (GL) theory, we first show that for pairing governed by the E_u representation, a nematic-to-chiral phase transition occurs at a critical chemical potential. Consider the ground state of the E_u representation with the order parameter

$$\mathbf{d}(\mathbf{p}_F) = \eta_1 \mathbf{d}_1^{E_u}(\mathbf{p}_F) + \eta_2 \mathbf{d}_2^{E_u}(\mathbf{p}_F). \quad (\text{S18})$$

The GL free energy up to fourth order is then given by

$$\mathcal{F} = \alpha |\boldsymbol{\eta}|^2 + \beta_1 |\boldsymbol{\eta}|^4 + \beta_2 |\eta_1 \eta_2^* - \eta_1^* \eta_2|^2. \quad (\text{S19})$$

The thermodynamic stability of superconducting states below T_c requires $\alpha \propto T - T_c$ and $\beta_1 > 0$. The fourth-order coefficient defined as

$$\beta_2 = -\langle (\mathbf{d}_1 \cdot \mathbf{d}_2)^2 \rangle_{\text{FS}} + \langle (\mathbf{d}_1 \times \mathbf{d}_2)^2 \rangle_{\text{FS}}, \quad (\text{S20})$$

determines the order parameter configuration $\boldsymbol{\eta} = (\eta_1, \eta_2)$, where $\langle \dots \rangle_{\text{FS}} \equiv \int dS_p \dots$ is an average over the Fermi surface that satisfies $\int dS_p = 1$.

For $\beta_2 > 0$, the nematic state with $(\eta_1, \eta_2) = \Delta(\cos \vartheta, \sin \vartheta)$ is stable as the highly degenerate minima of \mathcal{F} with respect to $\vartheta \in [0, \pi/2]$. The gap structure has two point nodes in the xy plane [Fig. 1(a) in the main text]. The continuous degeneracy with respect to ϑ is accidental, and is lifted by the sixth-order term representing the hexagonal warping of the Fermi surface,

$$\mathcal{F}_6 = \kappa [(\eta_+^* \eta_-)^3 + (\eta_+ \eta_-^*)^3], \quad (\text{S21})$$

with $\eta_\pm \equiv \eta_1 \pm i\eta_2$, which pins the nematic angle ϑ to one of three equivalent crystal axes.

The $\beta_2 < 0$ region is covered by the chiral state, $(\eta_1, \eta_2) = \Delta(1, \pm i)$, which breaks time reversal symmetry. As a result of spin-orbit coupling, the chiral state, $\mathbf{d}_1 \pm i\mathbf{d}_2$, is also a nonunitary state, with two distinct gaps: fully gapped and a gap with point nodes at $\mathbf{p} = \pm p_{F,z} \hat{z}$.

In $M_x\text{Bi}_2\text{Se}_3$, the intercalation of M atoms between the quintuple layers modifies the c -axis length of the crystal, namely, the hopping parameters along the z -axis (c_1, m_1, v_z). To incorporate the Fermi surface evolution, we follow Ref. [46]: the set of parameters in Ref. [42] for $\mu = 0.4$ eV and the half-value of (c_1, m_1, v_z) for $\mu = 0.65$ eV. The parameters for arbitrary μ are given by interpolating (c_1, m_1, v_z) linearly with respect to μ (for the further information, see the next subsection). With this parametrization, the Fermi surface is opened along the z -axis for $\mu \gtrsim 0.5$ eV. Using this set of parameters, we calculate the β_2 as a function of μ . We find that there exists the critical value $\mu_c = 0.7$ eV at which $\beta_2 = 0$ corresponding to a nematic-to-chiral phase transition.

Nematicity and chirality modes: Time-dependent Ginzburg-Landau theory

To understand characteristic bosonic excitations in the nematic ground state, we first solve the time-dependent Ginzburg-Landau (TDGL) theory. Let $\eta(t)$ be a dynamical bosonic field representing the E_u order parameter. The equation of motion for $\eta(t)$ is obtained from the effective Lagrangian,

$$\mathcal{L} \equiv \tau |\partial_t \eta|^2 - \mathcal{F}[\eta_j, \eta_j^*] - \mathcal{F}_6[\eta_j, \eta_j^*], \quad (\text{S22})$$

with an effective inertia of Cooper pair fluctuations, $\tau > 0$. Although the effective Lagrangian formalism does not incorporate the contribution of Bogoliubov quasiparticles, it can quantitatively describe all the collective modes in the bulk superfluid $^3\text{He-B}$ [55, 62]. This also gives a tractable way to capture the bosonic excitations in unconventional SCs. We then introduce the linear fluctuation of the order parameter, $\delta\eta(t) \equiv \eta(t) - \eta$, in terms of two orthogonal nematic vectors, $\mathbf{b}_1 = (\cos \vartheta, \sin \vartheta)$ and $\mathbf{b}_2 = (-\sin \vartheta, \cos \vartheta)$, as

$$\delta\eta^C(t) = \mathcal{D}_1^C(t)\mathbf{b}_1 + \mathcal{D}_2^C(t)\mathbf{b}_2. \quad (\text{S23})$$

All the collective modes are separated to the four sectors. Two of them are in the ground state sector \mathcal{D}_1^C and the others are in the orthogonal sector \mathcal{D}_2^C , where

$$\mathcal{D}_j^C = \mathcal{D}_j + C\mathcal{D}_j^* \quad (\text{S24})$$

is the parity eigenstate under particle-hole conversion.

Consider the phase fluctuation of the equilibrium sector, $\mathbf{d}(t) = \Delta e^{i\delta\vartheta} \mathbf{d}_1^{E_u} \approx \Delta(1 + i\delta\vartheta) \mathbf{d}_1^{E_u}$. Then, the mode with $\mathcal{D}_1^- = i\Delta\delta\vartheta$ corresponds to the NG mode associated with the broken $U(1)_N$ symmetry, which is gapped out by the Anderson-Higgs mechanism. The amplitude fluctuation is represented by $\mathcal{D}_1^+ = \delta\epsilon(t)$, where $\mathbf{d}(t) = [\Delta + \delta\epsilon(t)] \mathbf{d}_1^{E_u}$. The fluctuation modes of the orthogonal basis to the equilibrium basis are represented by \mathcal{D}_2^C . Let us suppose $\mathcal{D}_2^+ = \mathcal{D}_2 + \mathcal{D}_2^* = \Delta\delta\vartheta(t)$ and $\mathcal{D}_2^- = \mathcal{D}_2 - \mathcal{D}_2^* = i\epsilon(t)\Delta$. Using these parameterizations, the \mathcal{D}_2^+ mode leads to $\mathbf{d}(t) = \Delta[\mathbf{d}_1^{E_u} + \delta\vartheta(t)\mathbf{d}_2^{E_u}]$, then $[\eta_1(t), \eta_2(t)] = [1, \delta\vartheta(t)] \approx [\cos(\delta\vartheta(t)), \sin(\delta\vartheta(t))]$ for $\delta\vartheta \ll 1$. This is the pseudo-NG mode associated with the broken rotation symmetry or the fluctuation of the nematic order. The \mathcal{D}_2^- mode gives rise to the fluctuation of the chirality or orbital angular momentum of Cooper pairs, $\mathbf{d}(t) = \Delta[\mathbf{d}_1^{E_u} + i\epsilon(t)\mathbf{d}_2^{E_u}]$. We term \mathcal{D}_2^+ and \mathcal{D}_2^- the nematicity mode and chiral Higgs mode, respectively.

The Euler-Lagrange equation is obtained from \mathcal{L} in Eq. (S22) as

$$-\partial_t^2 \mathcal{D}_j^C = \frac{1}{\tau} \frac{\delta^2 \mathcal{F}_{\text{GL}}}{\delta \mathcal{D}_j^C \delta \mathcal{D}_j^C} \equiv (M_j^C)^2 \mathcal{D}_j^C. \quad (\text{S25})$$

The mass gap of each bosonic mode, M_j^C , represents the local curvature of $\mathcal{F}_{\text{GL}} \equiv \mathcal{F} + \mathcal{F}_6$ around the GL equilibrium solution. The mass gap of the chiral Higgs mode is given by

$$M_{E_u,2}^- = \Delta \sqrt{2(\beta_2 + 3\kappa\Delta^2)/\tau}. \quad (\text{S26})$$

The nematicity mode, which is the NG mode associated with the nematic order, is gapped out by explicit symmetry breaking due to the hexagonal warping effect as

$$M_{E_u,2}^+ = 6\Delta^2 \sqrt{2\kappa/\tau}. \quad (\text{S27})$$

For $\kappa = 0$, the mass gap of the chiral Higgs mode vanishes at $\beta_2 = 0$, corresponding to $\mu_c = 0.7$ eV. This softening of the chiral Higgs mode reflects that for $\beta_2 < 0$, i.e., $\mu > \mu_c$, the GL functional exhibits negative curvature around nematic ground state, i.e., the dynamical instability of the nematic state towards the chiral state.

We note that the TDGL theory does not incorporate the contribution of Bogoliubov quasiparticles. As the nodal structure of the nematic gap function changes from the point node to line node as μ increases, the quasiparticle contributions to the mass shift and damping of bosons become significant in the vicinity of the nematic-to-chiral phase transition. Below, using the quasiclassical Keldysh theory, we examine the mass shift and damping rate of the low-lying bosonic excitations in the nematic ground state. We demonstrate that thermally excited Bogoliubov quasiparticles lead to the significant mass shift in high temperatures, while the TDGL theory can qualitatively capture the characteristic bosonic modes in nematic SCs.

Nematic-to-chiral phase transition: Quasiclassical theory

Here we describe the self-consistent equations and thermodynamic potential in terms of the equilibrium propagator, $\hat{g}_0^M(\mathbf{p}_F, \varepsilon_n)$. The equilibrium propagator for unitary states, $\mathbf{d} \times \mathbf{d}^* = \mathbf{0}$, is

$$\hat{g}_0^M(\mathbf{p}_F, \varepsilon_n) = -\pi \frac{i\varepsilon_n \hat{\tau}_3 - \hat{\Delta}(\mathbf{p}_F)}{\sqrt{\varepsilon_n^2 + |\mathbf{d}(\mathbf{p}_F)|^2}}, \quad (\text{S28})$$

where

$$\hat{\Delta}(\mathbf{p}_F) \equiv \begin{pmatrix} 0 & i\sigma_\mu \sigma_2 d_\mu(\mathbf{p}_F) \\ i\sigma_2 \sigma_\mu d_\mu^*(\mathbf{p}_F) & 0 \end{pmatrix}. \quad (\text{S29})$$

is the equilibrium superconducting order parameter matrix in the Nambu space. For non-unitary states, $\mathbf{q} \equiv i\mathbf{d} \times \mathbf{d}^* \neq \mathbf{0}$, the spin-triplet components of the anomalous propagator are given by

$$f^M(\mathbf{p}_F, \varepsilon_n) = \frac{\sqrt{2}\alpha}{1 - \alpha^2 q^2} [\mathbf{d} + i\alpha \mathbf{d} \times \mathbf{q}], \quad (\text{S30})$$

where

$$\alpha(\mathbf{p}_F, \varepsilon_n) \equiv \frac{1}{\varepsilon_n^2 + |\mathbf{d}(\mathbf{p}_F)|^2 + \sqrt{[\varepsilon_n^2 + |\mathbf{d}(\mathbf{p}_F)|^2]^2 - [\mathbf{q}(\mathbf{p}_F)]^2}}. \quad (\text{S31})$$

These propagators obey the normalization condition $[\hat{g}_0^M(\mathbf{p}_F, \varepsilon_n)]^2 = -\pi^2$.

The pair potential, (η_1, η_2) , at the temperature T is determined by solving the gap equation

$$d_\mu(\mathbf{p}_F) = T \sum_{|\varepsilon_n| < \varepsilon_{n,c}} \langle V_{\mu\nu}(\mathbf{p}_F, \mathbf{p}'_F) f_\nu(\mathbf{p}'_F, \varepsilon_n) \rangle'_{\text{FS}} \quad (\text{S32})$$

where $\langle \dots \rangle_{\text{FS}} = \int dS_{\mathbf{p}} \dots$ is an average over the Fermi surface that satisfies $\int dS_{\mathbf{p}} = 1$. In the nematic state, the gap equation is recast into

$$\frac{1}{V(E_u)} = \pi T \sum_{|\varepsilon_n| < \varepsilon_{n,c}} \left\langle \frac{|d_1^{(E_u)}(\mathbf{p}_F)|^2}{\sqrt{\varepsilon_n^2 + |d(\mathbf{p}_F)|^2}} \right\rangle_{\text{FS}}. \quad (\text{S33})$$

We here assume the separable form of the pairing interaction

$$V_{\mu\nu}(\mathbf{p}_F, \mathbf{p}'_F) = - \sum_{\Gamma} \sum_{j=1}^{n_{\Gamma}} V_j^{(\Gamma)} d_{\mu,j}^{(\Gamma)}(\mathbf{p}_F) d_{\nu,j}^{(\Gamma)*}(\mathbf{p}'_F), \quad (\text{S34})$$

which comprises attractive interactions ($V_j^{(\Gamma)} > 0$) in the irreducible representations of the symmetry group D_{3d} , $\Gamma = \{A_{1g}, A_{1u}, A_{2u}, E_u\}$. In calculating Eq. (S33), we utilize the fact that ε_c and $V^{(\Gamma)}$ are related to measurable quantity, the bulk transition temperature T_c , by linearized gap equation

$$\frac{1}{V_1^{(E_u)}} = \langle |d_1^{(E_u)}(\mathbf{p}_F)|^2 \rangle_{\text{FS}} K(T), \quad (\text{S35})$$

where $K(T)$ is the digamma function of argument $\varepsilon_c/2\pi T \gg 1$,

$$K(T) = \pi T \sum_{|\varepsilon_n| < \varepsilon_c} \frac{1}{|\varepsilon_n|} \approx \ln \frac{1.13\varepsilon_c}{T}. \quad (\text{S36})$$

This relation can be utilized to eliminate ε_c and $V_1^{(E_u)}$ from the gap equation, and Eq. (S33) reduces to

$$\langle D \rangle_{\text{FS}} \ln \frac{T}{T_c} = \pi T \sum_n \left\langle \frac{D}{\sqrt{\varepsilon_n^2 + |d|^2}} - \frac{D}{|\varepsilon_n|} \right\rangle_{\text{FS}}, \quad (\text{S37})$$

which is free from the ultraviolet divergence. In the same way, the gap equation for the non-unitary chiral state is given by

$$\begin{aligned} \langle D \rangle_{\text{FS}} \ln \frac{T}{T_c} = \pi T \sum_n \left\langle \frac{\sqrt{2\alpha}}{1 - \alpha^2 q^2} \right. \\ \left. \times \left\{ D + \alpha \Delta^2 (|d_1^{E_u} \cdot d_2^{E_u}|^2 - |d_1^{E_u}|^2 |d_2^{E_u}|^2) \right\} - \frac{D}{|\varepsilon_n|} \right\rangle_{\text{FS}}. \end{aligned} \quad (\text{S38})$$

Here we set $D \equiv |d_1^{E_u}|^2$ for the nematic state and $D \equiv (|d_1^{E_u}|^2 + |d_2^{E_u}|^2)/2$ for the chiral state. We solve the gap equations (S37) and (S38) to obtain the self-consistent solution of $\Delta(T)$ for the nematic and chiral states at a given μ and T .

To compute the phase diagram of superconducting topological insulators, we need to introduce a free energy functional in terms of the equilibrium quasiclassical propagators and self-consistent pair potentials. Following Ref. 63 and using the Luttinger-Ward functional formalism, we obtain the free energy functional relative to the normal state as

$$\begin{aligned} \Delta\Omega = N_F \langle |d|^2 \rangle \ln \frac{T}{T_c} \\ - N_F \int_0^1 d\lambda T \sum_n \left[\langle d \cdot \tilde{f}_{\lambda}^M + d^* \cdot \tilde{f}_{\lambda}^{M*} \rangle - \frac{\langle |d|^2 \rangle}{|\varepsilon_n|^2} \right] \end{aligned} \quad (\text{S39})$$

where \tilde{f}_{λ} is obtained from Eqs. (S28) and (S30) with replacing d to λd .

We first solve the gap equations (S37) and (S38) for the nematic and chiral state at (T, μ) , respectively. Then we calculate the thermodynamic potential, $\Delta\Omega$, with the gap functions and the anomalous propagators and compute the phase diagram presented in the main text. Here we utilize the set of parameters for $\mu = 0.4\text{eV}$ [42]: $m_0 = -0.28\text{eV}$, $m_1/c^2 = 0.216\text{eV}$, $m_2/a^2 = 56.6\text{eV}$, $v_z/c = 0.32\text{eV}$, and $v/a = 0.56\text{eV}$, where $a = 4.076\text{\AA}$ and $c = 29.830\text{\AA}$ are the lattice constants of the parent material. For $\mu = 0.65\text{eV}$, we set the half-value of (c_1, m_1, v_z) , and the parameters for arbitrary μ are given by interpolating (c_1, m_1, v_z) linearly with respect to μ . The linear interpolation models the Fermi surface evolution of doped Bi_2Se_3 , and the Fermi surface is opened along the z -axis for $\mu \gtrsim 0.5\text{eV}$. In Fig. S1, we show the free energies of the nematic and chiral states in the superconducting topological insulators $M_x\text{Bi}_2\text{Se}_3$.

Solutions of linear response functions

To linear order in $\delta\hat{g}^M$ the normalization condition for the non-equilibrium correction to the propagator becomes

$$\hat{g}_0^M(\varepsilon_n + \omega_m) \delta\hat{g}^M(\varepsilon_n, \omega_m) + \delta\hat{g}^M(\varepsilon_n, \omega_m) \hat{g}_0^M(\varepsilon_n) = 0, \quad (\text{S40})$$

where we use ε_n (ω_m) for the Matsubara frequency for fermions (bosons). Thus, we set $\varepsilon_{n_1} = \varepsilon_n + \omega_m$, $\varepsilon_{n_2} = \varepsilon_n$, and $\delta\hat{g}^M(\mathbf{p}_F, \mathbf{q}; \varepsilon_{n_1}, \varepsilon_{n_2}) \equiv \delta\hat{g}^M(\mathbf{p}_F, \mathbf{q}; \varepsilon_n, \omega_m)$. Substituting Eq. (S8) into Eq. (S3), the linearized transport equation for the non-equilibrium Matsubara propagator is given by

$$\begin{aligned} \{i(\varepsilon_n + \omega_m)\hat{\tau}_3 - \hat{\Delta}(\mathbf{p}_F)\} \delta\hat{g}^M - \delta\hat{g}^M \{i\varepsilon_n\hat{\tau}_3 - \hat{\Delta}(\mathbf{p}_F)\} - \eta\delta\hat{g}^M \\ + \hat{g}_0^M(\varepsilon_n + \omega_m)\delta\hat{h} - \delta\hat{h}\hat{g}_0^M(\varepsilon_n) = 0, \end{aligned} \quad (\text{S41})$$

where $\delta\hat{h} \equiv \hat{h} - \hat{\Delta}$. For unitary states, we solve this equation using the normalization condition (S40) and the solutions for g_0 in Eq. (S28). The linear response of the Matsubara

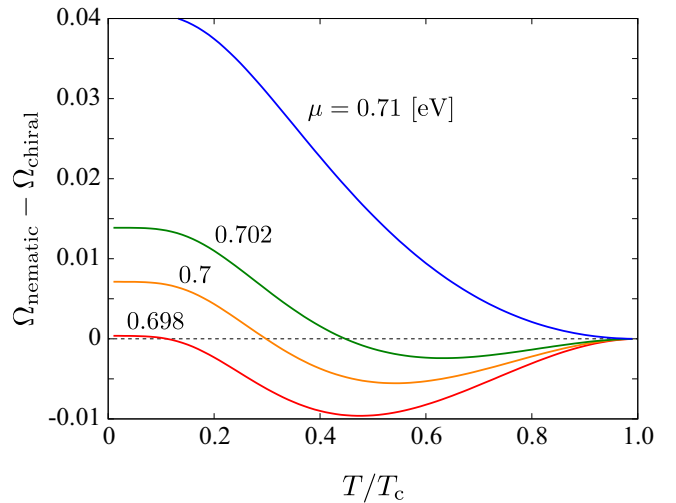


FIG. S1. Free energies of the nematic and chiral states for various μ in the vicinity of the nematic-chiral phase transition.

propagator is then given by

$$\delta\hat{g}^M = \frac{1}{D_+^2 + \eta^2} \left[\frac{D_+}{\pi} \left\{ \hat{g}_0^M(\varepsilon_n + \omega_m) \delta\hat{h}\hat{g}_0^M(\varepsilon_n) + \pi^2 \delta\hat{h} \right\} - \eta \left\{ +\delta\hat{h}\hat{g}_0^M(\varepsilon_n) - \hat{g}_0^M(\varepsilon_n + \omega_m) \delta\hat{h} \right\} \right], \quad (S42)$$

where $D(\mathbf{p}_F, \varepsilon_n) = \sqrt{\varepsilon_n^2 + |\mathbf{d}(\mathbf{p}_F)|^2}$ and $D_+(\varepsilon_n, \omega_m) \equiv D(\varepsilon_n + \omega_m) + D(\varepsilon_n)$.

For time-reversal invariant ground states with $\mathbf{d} \in \mathbb{R}^3$, the diagonal component of the quasiclassical Keldysh propagator becomes

$$\delta g_0^- = \frac{\omega\eta}{\omega^2 - \eta^2} (1 - \lambda) \Sigma_0^+ + \left\{ 1 + \frac{\eta^2}{\omega^2 - \eta^2} (1 - \lambda) \right\} \delta \Sigma_0^- + \frac{1}{2} \eta \bar{\lambda} d_\mu \delta d_\mu^-, \quad (S43)$$

and

$$\delta g^+ = \frac{\omega^2}{\omega^2 - \eta^2} (1 - \lambda) \Sigma^+ + \bar{\lambda} (\mathbf{d} \cdot \Sigma^+) \mathbf{d} + \frac{\omega\eta}{\omega^2 - \eta^2} (1 - \lambda) \Sigma^- - \frac{i}{2} \omega \bar{\lambda} \mathbf{d} \times \delta \mathbf{d}^+, \quad (S44)$$

where $\delta d_\mu^\pm \equiv \delta d_\mu \pm \delta d_\mu^*$, $\delta g_0^\pm \equiv \delta g_0 \pm \delta \bar{g}_0$, and $\delta \mathbf{g}^\pm \equiv \delta \mathbf{g} \pm \delta \bar{\mathbf{g}}$. Similarly, the anomalous Keldysh propagators, $\delta f_\mu^\pm = \delta f_\mu \pm \delta \bar{f}_\mu$, are given by

$$\delta f^- = \left\{ \frac{\gamma}{2} + \frac{1}{4} \bar{\lambda} (\omega^2 - 4|\mathbf{d}(\mathbf{p}_F)|^2 - \eta^2) \right\} \delta d^- + \bar{\lambda} \mathbf{d} [\mathbf{d} \cdot \delta d^-] - \frac{1}{2} \bar{\lambda} \mathbf{d} (\eta \delta \Sigma_0^- + \omega \delta \Sigma_0^+), \quad (S45)$$

and

$$\delta f^+ = \left\{ \frac{\gamma}{2} + \frac{1}{4} \bar{\lambda} (\omega^2 - \eta^2) \right\} \delta d^+ - \bar{\lambda} \mathbf{d} [\mathbf{d} \cdot \delta d^+] + \frac{i}{2} \bar{\lambda} \{ \eta (\mathbf{d} \times \delta \Sigma^-) + \omega (\mathbf{d} \times \delta \Sigma^+) \}. \quad (S46)$$

Here we introduce the bosonic response functions

$$\gamma(\omega_m) = \pi T \sum_{|\varepsilon_n| < \varepsilon_{n,c}} \left[\frac{1}{D(\varepsilon_n + \omega_m)} + \frac{1}{D(\varepsilon_n)} \right], \quad (S47)$$

$$\lambda(\omega_m) = \pi T \sum_{|\varepsilon_n| < \varepsilon_{n,c}} \frac{1}{D_+ D(\varepsilon_n + \omega_m) D(\varepsilon_n)}. \quad (S48)$$

Analytic continuation to real frequencies of $\gamma(\omega_m)$ in the manner of Eq. (S5) leads to

$$\gamma(\mathbf{p}_F) = 2 \int_{|\mathbf{d}|}^{\varepsilon_c} d\varepsilon \frac{1}{\sqrt{\varepsilon^2 - |\mathbf{d}|^2}} \tanh\left(\frac{\varepsilon}{2T}\right), \quad (S49)$$

where the frequency dependence can be ignored for $\omega_m \ll \varepsilon_c$. The γ -function is related to the equilibrium gap equation (S33)

$$\frac{1}{V(E_u)} = \frac{1}{2} \left\langle \gamma(\mathbf{p}_F) |\mathbf{d}_1^{(E_u)}(\mathbf{p}_F)|^2 \right\rangle_{\text{FS}}. \quad (S50)$$

The analytic continuation of $\lambda(\omega_m)$ yields the generalized Tsuneto function, $\lambda(\mathbf{p}_F, \mathbf{Q}, \omega) = |\mathbf{d}(\mathbf{p}_F)|^2 \bar{\lambda}(\mathbf{p}_F, \mathbf{Q}, \omega)$,

$$\lambda = |\mathbf{d}|^2 \int_{|\mathbf{d}|}^{\varepsilon_c} d\varepsilon \frac{2 \tanh(\varepsilon/2T)}{\sqrt{\varepsilon^2 - |\mathbf{d}|^2}} \left[\frac{\eta^2 - 2\omega\varepsilon_+}{(4\varepsilon_+^2 - \eta^2)(\omega^2 - \eta^2) + 4\eta^2|\mathbf{d}|^2} + \frac{\eta^2 + 2\omega\varepsilon_-}{(4\varepsilon_-^2 - \eta^2)(\omega^2 - \eta^2) + 4\eta^2|\mathbf{d}|^2} \right], \quad (S51)$$

where $\varepsilon_\pm \equiv \varepsilon \pm \omega/2$. The generalized Tsuneto function represents the “stiffness” of the condensate at the temperature T and frequency ω and yields the momentum dependence in the nematic state. In the long-wavelength limit, the Tsuneto function reduces to

$$\lambda(\mathbf{p}_F, \omega) = \int_{|\mathbf{d}(\mathbf{p}_F)|}^{\varepsilon_c} \frac{|\mathbf{d}(\mathbf{p}_F)|^2 d\varepsilon}{\sqrt{\varepsilon^2 - |\mathbf{d}(\mathbf{p}_F)|^2}} \left\{ \frac{\tanh(\varepsilon/2T)}{\varepsilon^2 - \omega^2/4} \right\} + O(\eta^2), \quad (S52)$$

with $\varepsilon_c \rightarrow \infty$. By introducing new variable, $\xi = \sqrt{\varepsilon^2 - |\mathbf{d}|^2}$ and utilizing the series expansion

$$\frac{\tanh(x/2T)}{2x} = T \sum_{\varepsilon_n} \frac{1}{\varepsilon_n^2 + x^2}, \quad (S53)$$

the Tsuneto function is rewritten in terms of the Matsubara sum

$$\lambda(\mathbf{p}_F, \omega) = \frac{\pi}{2} \left(\frac{2|\mathbf{d}(\mathbf{p}_F)|}{\omega} \right) \frac{\tanh(\omega/4T)}{\sqrt{1 - (\omega/2|\mathbf{d}(\mathbf{p}_F)|)^2}} - T \sum_{|\varepsilon_n| < \varepsilon_{n,c}} \frac{\pi |\mathbf{d}(\mathbf{p}_F)|^2}{(\varepsilon_n^2 + \omega^2/4) \sqrt{\varepsilon_n^2 + |\mathbf{d}(\mathbf{p}_F)|^2}}, \quad (S54)$$

for $\omega < 2|\mathbf{d}(\mathbf{p}_F)|$. Above the pair-breaking frequency, $\omega > 2|\mathbf{d}(\mathbf{p}_F)|$, the Tsuneto function acquires an imaginary part

$$\lambda(\mathbf{p}_F, \omega) = -T \sum_{|\varepsilon_n| < \varepsilon_{n,c}} \frac{\pi |\mathbf{d}(\mathbf{p}_F)|^2}{(\varepsilon_n^2 + \omega^2/4) \sqrt{\varepsilon_n^2 + |\mathbf{d}(\mathbf{p}_F)|^2}} + i \frac{\pi}{2} \left(\frac{2|\mathbf{d}(\mathbf{p}_F)|}{\omega} \right) \frac{\tanh(\omega/4T)}{\sqrt{(\omega/2|\mathbf{d}(\mathbf{p}_F)|)^2 - 1}}. \quad (S55)$$

The imaginary part, $\text{Im}\lambda > 0$, reflects the density of pair excitations of Bogoliubov quasiparticles and gives rise to the damping of collective modes.

In the zero-temperature, long-wavelength limit, the Tsuneto function is recast into

$$\lambda(x) = \frac{\sin^{-1}(x)}{x \sqrt{1 - x^2}}, \quad (S56)$$

for $|x| \equiv |\omega/2|\mathbf{d}(\mathbf{p}_F)| < 1$ and

$$\lambda(x) = -\frac{\ln(x + \sqrt{x^2 - 1})}{x \sqrt{x^2 - 1}} + \frac{i\pi}{2x \sqrt{x^2 - 1}} \quad (S57)$$

for $|x| > 1$.

S2. ORDER PARAMETER FLUCTUATIONS

For time-reversal invariant superconductors with $\mathbf{d} \in \mathbb{R}^3$, the order parameter fluctuations, $\delta d_\mu \equiv \delta d_\mu(\mathbf{p}_F, \mathbf{Q}, \omega)$, are obtained from the non-equilibrium gap equations

$$\delta d_\mu(\mathbf{p}_F, \mathbf{Q}, \omega) = - \left\langle \int \frac{d\varepsilon}{4\pi i} V_{\mu\nu}(\mathbf{p}_F, \mathbf{p}'_F) \delta f_\nu(\mathbf{p}'_F, \varepsilon; \mathbf{Q}, \omega) \right\rangle_{\text{FS}} \quad (S58)$$

and Eqs. (S45) and (S46) as

$$\delta d_\mu^- = - \left\langle V_{\mu\nu}(\mathbf{p}_F, \mathbf{p}'_F) \left\{ \frac{\gamma}{2} \delta d_\nu^- + \frac{1}{4} \bar{\lambda} (\omega^2 - 4|\mathbf{d}|^2 - \eta^2) \delta d_\nu^- + \bar{\lambda} d_\nu \delta d_\eta^- - \frac{1}{2} \bar{\lambda} d_\nu (\eta \delta \Sigma_0^- + \omega \delta \Sigma_0^+) \right\} \right\rangle_{\text{FS}}, \quad (S59)$$

and

$$\delta d_\mu^+ = - \left\langle V_{\mu\nu}(\mathbf{p}_F, \mathbf{p}_F') \left\{ \frac{\gamma}{2} \delta d_\nu^+ + \frac{1}{4} \bar{\lambda} (\omega^2 - \eta^2) \delta d_\nu^+ - \bar{\lambda} d_\nu d_\eta \delta d_\eta^+ \right\} + \frac{i}{2} \bar{\lambda} \epsilon_{\eta\tau} (\eta d_\nu \delta \Sigma_\tau^- + \omega d_\nu \delta \Sigma_\tau^+) \right\rangle'_{\text{FS}}, \quad (\text{S60})$$

The last terms in Eq. (S59) and (S60) represents an external source field that drives the order parameter fluctuations.

Consider the E_u state represented in Eq. (S18). We now expand the order parameter fluctuation in terms of the (Γ, j) basis functions, $\mathbf{d}_j^{(\Gamma)}(\mathbf{p}_F)$, as

$$\delta d_\nu(\mathbf{p}_F, \mathbf{Q}, t) = \sum_{\Gamma} \sum_{j=1}^{\text{odd } n_\Gamma} \mathcal{D}_{\Gamma,j}^C(\mathbf{Q}, t) \mathbf{d}_j^{(\Gamma)}(\mathbf{p}_F) \quad (\text{S61})$$

where $\Gamma = \{A_{1u}, A_{2u}, E_u\}$ are the odd-parity irreducible representation of the crystal symmetry D_{3d} and n_Γ is the dimension of Γ . Substituting this into Eqs. (S59) and (S60) and ignoring the external source terms, one obtains the

equations of motion for $C = \pm$ normal modes

$$\left[\frac{\bar{\lambda}_{\Gamma,j}}{4} \omega^2 - \mathbb{M}_{\Gamma,j}^C(\mathbf{Q}, \omega) \right] \mathcal{D}_{\Gamma,j}^C(\mathbf{Q}, \omega) = 0, \quad (\text{S62})$$

which are the nonlinear equations on ω . The excitation gaps are determined by

$$\frac{\bar{\lambda}_{\Gamma,j}}{4} \omega^2 - \mathbb{M}_{\Gamma,j}^- \equiv \left[-\frac{1}{V_j^{(\Gamma)}} + \left\langle \left\{ \frac{\gamma}{2} + \frac{\bar{\lambda}}{4} (\omega^2 - 4|\mathbf{d}|^2 - \eta^2) \right\} |\mathbf{d}_j^{(\Gamma)}|^2 \right\rangle_{\text{FS}} + \left\langle \bar{\lambda} |\mathbf{d} \cdot \mathbf{d}_j^{(\Gamma)}|^2 \right\rangle_{\text{FS}} \right] = 0, \quad (\text{S63})$$

for $C = -$ and

$$\frac{\bar{\lambda}_{\Gamma,j}}{4} \omega^2 - \mathbb{M}_{\Gamma,j}^+ \equiv \left[-\frac{1}{V_j^{(\Gamma)}} + \left\langle \left\{ \frac{\gamma}{2} + \frac{\bar{\lambda}}{4} (\omega^2 - \eta^2) \right\} |\mathbf{d}_j^{(\Gamma)}|^2 \right\rangle_{\text{FS}} - \left\langle \bar{\lambda} |\mathbf{d} \cdot \mathbf{d}_j^{(\Gamma)}|^2 \right\rangle_{\text{FS}} \right] = 0, \quad (\text{S64})$$

for $C = +$, where we have introduced $\bar{\lambda}_{\Gamma,j} \equiv \langle \bar{\lambda} |\mathbf{d}_j^{(\Gamma)}|^2 \rangle_{\text{FS}}$. Equations (S63) and (S64) are recast into

$$\frac{\bar{\lambda}_{\Gamma,j}}{4} \omega^2 - \left\langle |\mathbf{d}_j^{(\Gamma)}|^2 \right\rangle_{\text{FS}} \ln \frac{T}{T_c} - \pi T \sum_n \left\langle \frac{|\mathbf{d}_j^{(\Gamma)}|^2}{\sqrt{\varepsilon_n^2 + |\mathbf{d}|^2}} - \frac{|\mathbf{d}_j^{(\Gamma)}|^2}{|\varepsilon_n|} \right\rangle_{\text{FS}} \left\{ -\langle \lambda |\mathbf{d}_j^{(\Gamma)}|^2 \rangle_{\text{FS}} - \frac{1}{4} \langle \eta^2 \bar{\lambda} |\mathbf{d}_j^{(\Gamma)}|^2 \rangle_{\text{FS}} + \langle \bar{\lambda} |\mathbf{d} \cdot \mathbf{d}_j^{(\Gamma)}|^2 \rangle_{\text{FS}} + x_{\Gamma,j} \langle |\mathbf{d}_j^{(\Gamma)}|^2 \rangle_{\text{FS}} \right\} = 0, \quad (\text{S65})$$

for $C = -$ and

$$\frac{\bar{\lambda}_{\Gamma,j}}{4} \omega^2 - \left\langle |\mathbf{d}_j^{(\Gamma)}|^2 \right\rangle_{\text{FS}} \ln \frac{T}{T_c} - \pi T \sum_n \left\langle \frac{|\mathbf{d}_j^{(\Gamma)}|^2}{\sqrt{\varepsilon_n^2 + |\mathbf{d}|^2}} - \frac{|\mathbf{d}_j^{(\Gamma)}|^2}{|\varepsilon_n|} \right\rangle_{\text{FS}} \left\{ -\frac{1}{4} \langle \eta^2 \bar{\lambda} |\mathbf{d}_j^{(\Gamma)}|^2 \rangle_{\text{FS}} - \langle \bar{\lambda} |\mathbf{d} \cdot \mathbf{d}_j^{(\Gamma)}|^2 \rangle_{\text{FS}} + x_{\Gamma,j} \langle |\mathbf{d}_j^{(\Gamma)}|^2 \rangle_{\text{FS}} \right\} = 0, \quad (\text{S66})$$

for $C = +$.

Here we have introduced the parameter

$$x_{\Gamma,j} = \ln T_c^{(\Gamma,j)} / T_c < 0, \quad (\text{S67})$$

which represents the splitting of the critical temperature of the (Γ, j) attractive interaction channel relative to the that of the ground state $T_c = T_c^{(E_u,1)}$. The coupling constant, $1/V_j^{(E_u)}$, is obtained from Eq. (S50) and related to the measurable quantity, $T_c \equiv T_c^{E_u,1}$ by solving Eq. (S50) at $T = T_c$. The coupling constants in A_{1u} and A_{2u} channels, $1/V_j^{(A_{1u})}$ and $1/V_j^{(A_{2u})}$, are related to $T_c^{(A_{1u})}$ and $T_c^{(A_{2u})}$ by the gap equations which are obtained from Eq. (S50) by replacing $V^{(E_u)}$ with $V^{(A_{1u})}$ and $V^{(A_{2u})}$. Although both the Fermi surface average of the γ function and $1/V_j^{(\Gamma)}$ depend on the cutoff of the Matsubara frequencies, ε_c , their ultraviolet divergences are canceled out by each other, when ε_c is sufficiently large. Therefore, the resulting equations (S65) and (S66) are free from divergence in ε_c .

Equations (S65) and (S66) determine the eigenfrequencies of (Γ, j) bosonic modes in the nematic ground state, where we consider $\mathbf{d}(\mathbf{p}_F) = \Delta \mathbf{d}_1^{(E_u)}(\mathbf{p}_F)$ with $(\eta_1, \eta_2) = (1, 0)$ without loss of generality. We note that for $(\Gamma, j) = (E_u, 1)$, Eq. (S65) has a pole at $Q = 0$, i.e., $\mathbf{Q} = \mathbf{0}$ and

$\omega = 0$

$$\omega^2 = \frac{\langle (\hat{\mathbf{v}}_F \cdot \hat{\mathbf{Q}})^2 \bar{\lambda}(\mathbf{p}_F) |\mathbf{d}_1^{(E_u)}|^2 \rangle_{\text{FS}}}{\langle \bar{\lambda}(\mathbf{p}_F) |\mathbf{d}_1^{(E_u)}|^2 \rangle_{\text{FS}}} v_F^2 Q^2, \quad (\text{S68})$$

corresponding to the NG mode associated with $U(1)_N$ symmetry breaking. Here we have introduced $\hat{\mathbf{v}}_F \equiv \mathbf{v}_F/|\mathbf{v}_F|$ and $\hat{\mathbf{Q}} \equiv \mathbf{Q}/|Q|$.

Figure S2 shows the temperature and chemical potential dependences of the mass gaps of the chirality mode $\text{Re}M_{E_u,2}^-$ and the nematicity mode $\text{Re}M_{E_u,2}^+$. Here we set $x_{E_u,2} = 0$, i.e., $T_c^{E_u,2} = T_c^{E_u,1} = T_c$. The nematicity mode acquires the finite mass gap at finite temperatures. The T -dependence resembles that of the “normal-flapping mode” in the superfluid $^3\text{He-A}$ which is a vibration of the nodal direction about its equilibrium. The effective mass of such vibration mode is attributed to viscosity associated with the quasiparticle distribution around the gap nodes. Reflecting the density of the quasiparticles, the mass gap of the nematicity mode goes to zero with decreasing T . The damping rates of both the chirality and nematicity modes are shown in Fig. S3. We find that the damping rates satisfy $-\text{Im}M/\text{Re}M < 0.2$ for $T < T_c$ for all μ and thus the chirality (nematicity) mode involves the stable vibration of

the chirality of the Cooper pairs (the nodal direction or the nematicity angle) as long as $\text{Re}M > 0$. The increase of the damping rate of the nematicity mode with increasing μ reflects the increase of the quasiparticle density due to the evolution of the gap structure from the point nodes to line nodes.

S3. CURRENT RESPONSE AND POWER ABSORPTION

We now consider the response to an electromagnetic field,

$$\delta\Sigma_0(\mathbf{p}_F, \mathbf{Q}, \omega) = -\frac{e}{c}\mathbf{v}_F \cdot \mathbf{A}(\mathbf{Q}, \omega), \quad (\text{S69})$$

where $\mathbf{A}(\mathbf{Q}, \omega)$ is the vector potential. For the electromagnetic response of unconventional (spin-triplet) supercon-

ductors we focus on the collisionless regime, where impurity vertex corrections may be neglected. The current response contains contributions from the bosonic collective modes driven by the electromagnetic field, in addition to Bogoliubov quasiparticle contributions to the current. The current response is obtained from the diagonal component of the quasiclassical Keldysh propagator as

$$j_\mu(Q) = -2eN_F \left\langle v_F^\mu \int \frac{d\epsilon}{4\pi i} \delta g_0^-(\mathbf{p}_F, \mathbf{Q}; \epsilon, \omega) \right\rangle_{\text{FS}}. \quad (\text{S70})$$

The factor 2 originates in the spin degeneracy. Substituting the solution in Eq. (S43), one reads

$$j_\mu(Q) \equiv K_{\mu\nu}^{\text{QP}}(Q)A_\nu + K_{\mu\nu}^{\text{CM}}(Q)A_\nu. \quad (\text{S71})$$

The first term in Eq. (S71) is the contribution of quasiparticle (single-particle) excitations to the current

$$K_{\mu\nu}^{\text{QP}}(Q) = -\frac{2e^2N_F}{c} \left\langle \left\{ 1 + \frac{\eta^2}{\omega^2 - \eta^2} (1 - \lambda) \right\} v_F^\mu v_F^\nu \right\rangle_{\text{FS}}. \quad (\text{S72})$$

The another term in the current response is attributed to the contribution of the bosonic collective excitations. For time-reversal invariant superconducting states within the quasiclassical approximation ($T_c \ll T_F$), the electromagnetic wave can couple only to the $C = -$ modes, including the chirality mode in the nematic state. The current response is decomposed into contributions from chiral E_u , A_{1u} , and A_{2u} modes

$$K_{\mu\nu}^{\text{CM}}(Q) = K_{\mu\nu}^{(E_u,1)}(Q) + K_{\mu\nu}^{(E_u,2)}(Q) + K_{\mu\nu}^{(A_{1u})}(Q) + K_{\mu\nu}^{(A_{2u})}(Q), \quad (\text{S73})$$

where $K_{\mu\nu}^{(\Gamma,j)}(Q)$ represents contributions from $\mathcal{D}_{\Gamma,j}^-$ modes in the $(E_u, 1)$ nematic ground state to the response function,

$$K_{\mu\nu}^{(\Gamma,j)}(Q, \omega) = -2eN_F Q_\tau \sum_{j=1}^{n_\Gamma} \zeta_{\mu\tau}^{(\Gamma,j)}(Q, \omega) \frac{\delta \mathcal{D}_{\Gamma,j}^-(Q, \omega)}{\delta A_\nu}. \quad (\text{S74})$$

We now introduce the symmetric tensor

$$\zeta_{\mu\nu}^{(\Gamma,j)}(Q) = \Delta \left\langle \bar{\lambda}(\mathbf{p}_F, \mathbf{Q}, \omega) v_F^\mu v_F^\nu \mathbf{d}_1^{(E_u)}(\mathbf{p}_F) \cdot \mathbf{d}_j^{(\Gamma)}(\mathbf{p}_F) \right\rangle_{\text{FS}} \quad (\text{S75})$$

which determines the coupling of transverse EM waves with \mathbf{Q} and \mathbf{A} to the bosonic modes, $\mathcal{D}_{\Gamma,j}^-$, in the \mathbf{d}_i^Γ ground state. By using this tensor, the equation of motion for $\mathcal{D}_{\Gamma,j}^-$ is given as

$$\frac{\delta \mathcal{D}_{\Gamma,j}^-}{\delta A_\mu} = \left(\frac{e}{c} \right) \frac{Q_\nu \zeta_{\mu\nu}^{(\Gamma,j)}(Q)}{(\bar{\lambda}_{\Gamma,j}/4)\omega^2 - \mathbb{M}_{\Gamma,j}^-(Q)}. \quad (\text{S76})$$

The zeros of the denominator correspond to Eq. (S63) and determine the eigenfrequencies of (Γ, j) bosonic modes in the nematic ground state (see also Eq. (8) in the main text). To this end, the response function, $K_{\mu\nu}^{\text{CM}}(Q)$, reduces to

$$K_{\mu\nu}^{\text{CM}}(Q) = -\frac{e^2}{c} N_F \sum_{\Gamma}^{\text{odd}} \sum_{j=1}^{n_\Gamma} \frac{Q_\tau Q_\eta \zeta_{\mu\tau}^{(\Gamma,j)}(Q) \zeta_{\nu\eta}^{(\Gamma,j)}(Q)}{(\bar{\lambda}_{\Gamma,j}/4)\omega^2 - \mathbb{M}_{\Gamma,j}^-(Q)} \quad (\text{S77})$$

As we mention in the main text, ζ is subject to the symmetries of the equilibrium order parameter ($\mathbf{d}_1^{E_u}$) and dynamical bosonic field (\mathbf{d}_i^Γ). For the $E_{u,1}$ ground state, non-trivial components are $\zeta_{xy} = \zeta_{yx}$ for the chiral E_u mode

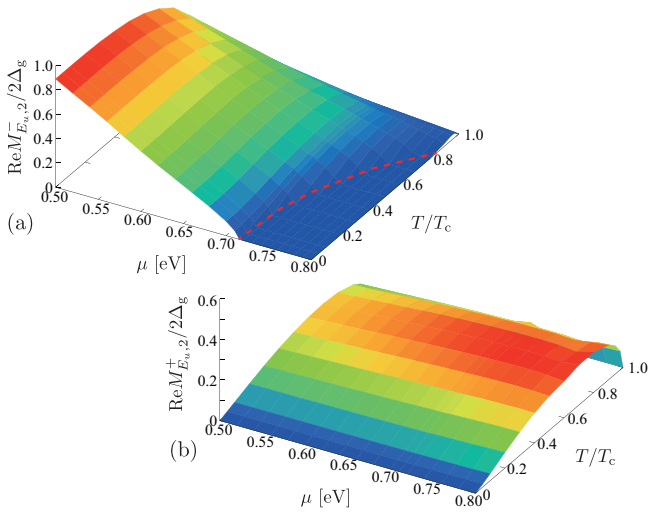


FIG. S2. Mass gap of the chirality mode $\text{Re}M_{Eu,2}^-$ (a) and the nematicity mode $\text{Re}M_{Eu,2}^+$ (b) for $x_{Eu,2} = 0$. The dashed curve corresponds to the dynamical instability of the chirality mode at which the mass gap closes, $\text{Re}M_{Eu,2}^- = 0$.

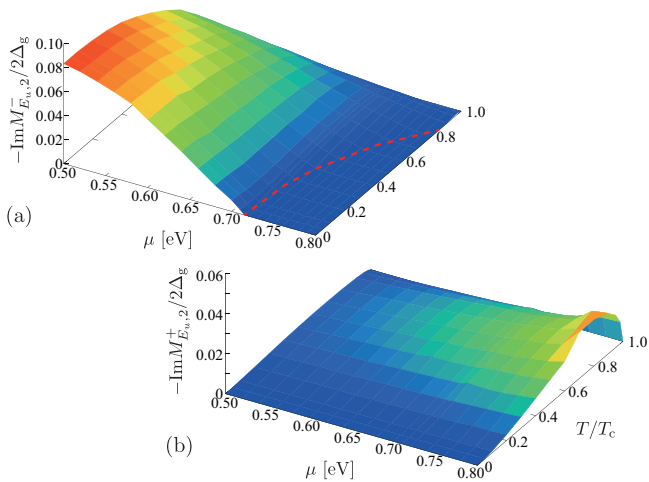


FIG. S3. Damping rate of the chirality mode $-\text{Im}M_{Eu,2}^-$ (a) and the nematicity mode $-\text{Im}M_{Eu,2}^+$ (b) for $x_{Eu,2} = 0$. The dashed curve corresponds to the dynamical instability of the chirality mode at which the mass gap closes, $\text{Re}M_{Eu,2}^- = 0$.

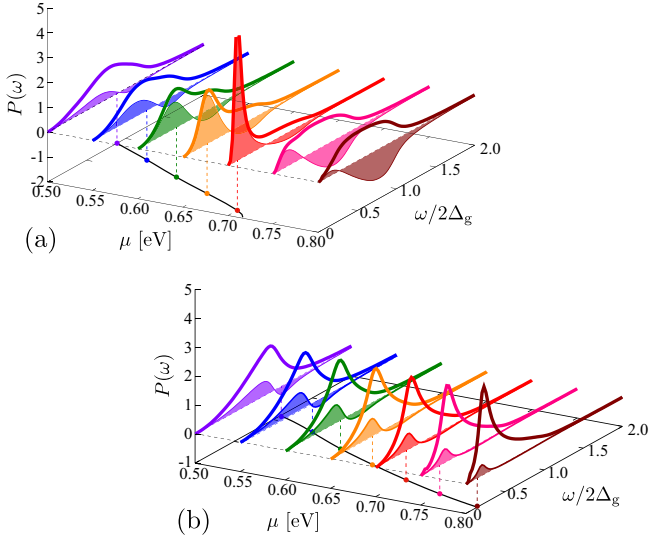


FIG. S4. Power absorption spectra, $P(\omega)$, in the nematic state with $d(\mathbf{p}_F) = \Delta(T, \mu) d_1^{E_u}(\mathbf{p}_F)$ for $T = 0.05T_c$: (a) $\mathbf{A} \parallel \mathbf{x}$ and $\mathbf{Q} \parallel \mathbf{y}$ and (b) $\mathbf{A} \parallel \mathbf{z}$ and $\mathbf{Q} \parallel \mathbf{y}$. The shaded are stands for the contributions of bosonic excitations, $P^{\text{CM}}(\omega)$. The mass gap of the chirality mode, $M_{E_u,2}^-$, and the A_{2u} mode, $M_{A_{2u}}^-$, are also shown in (a) and (b), respectively. We set $x_{E_u,2} = 0$ and $x_{A_{1u}} = x_{A_{2u}} = -1.5$, corresponding to $T_c^{(E_u,1)} = T_c^{(E_u,2)} = T_c$ and $T_c^{(A_{1u})} = T_c^{(A_{2u})} = 0.22T_c$.

$((\Gamma, i) = (E_u, 2))$ and $\zeta_{xz} = \zeta_{zx}$ for the chiral A_{2u} mode ($\Gamma = A_{2u}$). As $\mathbb{M}(\mathbf{Q})$ is subject to the enlarged D_∞ symmetry, the contribution from the chiral E_u mode to the response function is

$$K_{\mu\nu}^{(E_u,2)}(\mathbf{Q}) = \tilde{K}^{(E_u,2)}(\mathbf{Q}) \begin{pmatrix} \hat{Q}_y^2 & \hat{Q}_x \hat{Q}_y & 0 \\ \hat{Q}_x \hat{Q}_y & \hat{Q}_x^2 & 0 \\ 0 & 0 & 0 \end{pmatrix}. \quad (\text{S78})$$

Similarly, the contribution from the chiral A_{2u} mode reduces to

$$K_{\mu\nu}^{(A_{2u})}(\mathbf{Q}) = \begin{pmatrix} \tilde{K}_{xx}^{(A_{2u})}(\mathbf{Q}) \hat{Q}_z^2 & 0 & \tilde{K}_{xz}^{(A_{2u})}(\mathbf{Q}) \hat{Q}_x \hat{Q}_z \\ 0 & 0 & 0 \\ \tilde{K}_{zx}^{(A_{2u})}(\mathbf{Q}) \hat{Q}_z \hat{Q}_x & 0 & \tilde{K}_{zz}^{(A_{2u})}(\mathbf{Q}) \hat{Q}_x^2 \end{pmatrix} \quad (\text{S79})$$

The coupling of transverse EM fields to chiral A_{1u} modes is accidentally prohibited by the enlarged D_∞ symmetry, i.e., $K_{\mu\nu}^{(A_{1u})} = 0$.

The signatures of the collective mode spectrum are captured by the EM power absorption, which we calculate following the scheme in Ref. 23. Consider a metal-vacuum interface at $z = 0$, where $\hat{\mathbf{z}} \parallel \mathbf{Q}$ denotes the direction of the electromagnetic wave propagation is normal to the interface. The power absorption is obtained from Joule's law by integrating the energy density dissipated over the half space of the metal.

$$P(\omega) = \int_0^\infty dz \text{Re} [\mathbf{E}^*(\mathbf{r}, \omega) \cdot \mathbf{j}(\mathbf{r}, \omega)]. \quad (\text{S80})$$

Following Refs. 23 and 25, we map the half-space boundary-value problem with $\mathbf{B}(z = 0) = \mathbf{B}_0$ onto a full-space Maxwell equation with specular boundary condition at the interface. The electrons passing through the interface experience the mirror-reflected vector potential and magnetic field, as $\mathbf{A}(z) = \mathbf{A}(-z)$ and $\mathbf{B}(z) = -\mathbf{B}(-z)$.

Hence, the full-space Maxwell equation is accompanied by an external current sheet associated with the discontinuity of the field at the interface, $\mathbf{j}^{\text{ext}}(\omega) = -\frac{c}{2\pi} \mathbf{B}_0(\omega)$,

$$\left(\delta_{\mu\nu} \nabla^2 + \frac{4\pi}{c} K_{\mu\nu} \right) A_\nu = -\frac{4\pi}{c} j_\mu^{\text{ext}}, \quad (\text{S81})$$

where $K_{\mu\nu} \equiv K_{\mu\nu}^{\text{QP}} + K_{\mu\nu}^{\text{CM}}$ is the response function defined in Eq. (S71).

Let us consider the response of the $E_{u,1}$ ground state to transverse EM fields with $\mathbf{Q} \parallel \hat{\mathbf{x}}$. The current response is given as $\delta \mathbf{j} / \delta \mathbf{A} = (K^{\text{QP}} + \tilde{K}^{E_{u,2}}) \hat{\mathbf{y}} \equiv K \hat{\mathbf{y}}$ for $\mathbf{A} \parallel \hat{\mathbf{y}}$ and $\delta \mathbf{j} / \delta \mathbf{A} = (K^{\text{QP}} + \tilde{K}^{A_{2u}}) \hat{\mathbf{z}} \equiv K \hat{\mathbf{z}}$ for $\mathbf{A} \parallel \hat{\mathbf{z}}$. Solving for the Fourier component $\mathbf{A}(\mathbf{Q}, \omega)$, we have

$$\mathbf{A}(\mathbf{Q}, \omega) = -\frac{2B_0(\omega)}{Q^2 - (\frac{4\pi}{c})K(\mathbf{Q}, \omega)}. \quad (\text{S82})$$

Thus, the power absorption is given in terms of the response function as

$$P(\omega) = -\frac{2\omega|B_0(\omega)|^2}{c} \int_0^\infty \frac{dQ}{2\pi} \frac{\text{Im}K(\mathbf{Q}, \omega)}{|Q^2 - (\frac{4\pi}{c})K(\mathbf{Q}, \omega)|^2}. \quad (\text{S83})$$

Here we introduce the London penetration depth at $T = 0$

$$\Lambda = \sqrt{\frac{mc^2}{4\pi ne^2}}. \quad (\text{S84})$$

Then, the power absorption in Eq. (S83) is

$$P(\omega) = -\frac{\omega|B_0(\omega)|^2}{2\pi} \Lambda^2 \int_0^\infty \frac{dQ}{2\pi} \frac{\text{Im}K(\mathbf{Q}, \omega)}{|(Q\Lambda)^2 - \tilde{K}(\mathbf{Q}, \omega)|^2}. \quad (\text{S85})$$

The kernel is $\tilde{K} \approx \text{Re}(\tilde{K}) \approx -1$. The power absorption then becomes

$$P(\omega) \approx -\frac{\omega|B_0(\omega)|^2}{2\pi} \Lambda^2 \int_0^\infty \frac{dQ}{2\pi} \frac{\text{Im}K(\mathbf{Q}, \omega)}{|(Q\Lambda)^2 + 1|^2}. \quad (\text{S86})$$

Hence the power absorption reduces to the average of the dissipation part of the current kernel over the penetration depth $Q \lesssim \Lambda^{-1} < \xi^{-1}$. The quasiparticle and collective mode contributions of the power absorption are given as

$$P^{\text{QP}}(\omega) \approx -\frac{\omega|B_0(\omega)|^2}{2\pi} \Lambda^2 \int_0^\infty \frac{dQ}{2\pi} \frac{\text{Im}K^{\text{QP}}(\mathbf{Q}, \omega)}{|(Q\Lambda)^2 + 1|^2}, \quad (\text{S87})$$

$$P^{\text{CM}}(\omega) \approx -\frac{\omega|B_0(\omega)|^2}{2\pi} \Lambda^2 \int_0^\infty \frac{dQ}{2\pi} \frac{\text{Im}K^{\text{CM}}(\mathbf{Q}, \omega)}{|(Q\Lambda)^2 + 1|^2}. \quad (\text{S88})$$

In Fig. S4, we plot power absorption spectra, $P(\omega)$, in the nematic state at $T = 0.05T_c$. Figure S4 (a) and S4 (b) show the absorption of the transverse EM wave with ($\mathbf{A} \parallel \mathbf{x}, \mathbf{Q} \parallel \mathbf{y}$) and ($\mathbf{A} \parallel \mathbf{z}$ and $\mathbf{Q} \parallel \mathbf{y}$), respectively. The former case resonates the chirality mode $\mathcal{D}_{E_u,2}^-$, while the latter involves the resonance of the massive A_{2u} mode, $\mathcal{D}_{A_{2u}}^-$, where the shaded represents the contributions of bosonic excitations, $P^{\text{CM}}(\omega)$.

S4. DYNAMICAL SPIN SUSCEPTIBILITIES

In the quasiclassical theory which is reliable in the weak coupling limit $T_c/T_F \ll 1$, the $C = +$ sector of the bosonic

excitations including the nematicity mode cannot be coupled to transverse EM waves. We here demonstrate the impact of the nematicity vibration mode on the dynamical magnetic response of the nematic state. Let us consider a time-dependent field directly coupled to the magnetic moment of the electrons in nematic superconductors (e.g., rf-fields). The quasiclassical self-energies for the dynamical Zeeman term is obtained by projecting Eq. (S10) onto the conduction band as

$$\delta\Sigma_\mu(\mathbf{Q}, \omega) = \frac{1}{1 + F_0^a} \sum_{\mu=x,y,z} \frac{1}{2} g_\mu^{\text{eff}} \mu_B s_\mu H_\mu(\mathbf{Q}, \omega), \quad (\text{S89})$$

where F_0^a is the Fermi liquid parameter associated with the anti-symmetric spin-dependent channel of the quasiparticle scattering process. The effective g -factor of the conduction band electrons is given by

$$g_i^{\text{eff}} \equiv g_{i0} + g_{ix} \frac{m}{\sqrt{m^2 + v_z^2 f_z^2 + v^2 p_\parallel^2}} \approx g_{i0} + g_{ix}. \quad (\text{S90})$$

For the parent material, Bi_2Se_3 , the effective g -factor is strongly anisotropic as $g_x^{\text{eff}} = g_y^{\text{eff}} = -8.24$ and $g_z^{\text{eff}} = -50.8$.

The magnetic response of the system is described by the magnetization density which is obtained from the vectorial components of the diagonal propagators as

$$M_\mu(\mathbf{Q}, \omega) = M_{N,\mu}(\mathbf{Q}, \omega) + \frac{g_\mu^{\text{eff}} \mu_B \mathcal{N}_F}{1 + F_0^a} \left\langle \int \frac{d\varepsilon}{4\pi i} \delta g_\mu(\mathbf{p}_F, \mathbf{Q}; \varepsilon, \omega) \right\rangle_{\text{FS}}, \quad (\text{S91})$$

where the first term in the right-hand side is the magnetization in the normal state,

$$M_{N,\mu} = \frac{1}{2} \frac{(g_\mu^{\text{eff}} \mu_B)^2 \mathcal{N}_F}{1 + F_0^a} H_\mu. \quad (\text{S92})$$

Substituting Eq. (S44) into Eq. (S91), one finds that the dynamical spin susceptibilities are composed of two terms

$$\chi_{\mu\nu}(\mathbf{Q}, \omega) \equiv \frac{\delta M_\mu}{\delta H_\nu} = \chi_{\mu\nu}^{\text{QP}}(\mathbf{Q}, \omega) + \chi_{\mu\nu}^{\text{CM}}(\mathbf{Q}, \omega). \quad (\text{S93})$$

The first term corresponds to the contributions of Bogoliubov quasiparticles and equilibrium \mathbf{d} -vector,

$$\chi_{\mu\nu}^{\text{QP}} = \chi_N \left[\delta_{\mu\nu} \left\{ 1 + \frac{1}{1 + F_0^a} \left\langle \frac{\omega^2}{\omega^2 - \eta^2} (1 - \lambda) \right\rangle_{\text{FS}} \right\} + \frac{1}{1 + F_0^a} \langle \bar{\lambda} d_\mu d_\nu \rangle_{\text{FS}} \right]. \quad (\text{S94})$$

This reduces to the spin susceptibility of the equilibrium nematic state at $\mathbf{Q} \rightarrow \mathbf{0}$ and $\omega \rightarrow 0$.

For the nematic state of $M_x\text{Bi}_2\text{Se}_3$, only the diagonal components of the tensor remains nontrivial. The second term, $\chi_{\mu\nu}^{\text{CM}}$, describes the resonance of the bosonic excitations in the $C = +$ sector including the nematicity vibration mode,

$$\chi_{\mu\nu}^{\text{CM}} = -\frac{i}{4} \omega \sum_{\Gamma} \sum_{j=1}^{n_\Gamma} \left\langle \bar{\lambda} (\mathbf{d} \times \mathbf{d}_j^{(\Gamma)})_\mu \right\rangle_{\text{FS}} \left(\frac{\delta \mathcal{D}_{\Gamma,j}^+}{\delta H_\nu} \right). \quad (\text{S95})$$

Similarly with the coupling of the chirality mode to transverse EM waves, the nematicity mode leads to a pronounced peak of dynamical spin susceptibilities at the resonant frequency,

$$\frac{\delta \mathcal{D}_{\Gamma,j}^+}{\delta H_\nu} = -\frac{i}{2} g_\nu^{\text{eff}} \mu_B \omega \frac{\langle \bar{\lambda} (\mathbf{d} \times \mathbf{d}_j^{(\Gamma)})_\nu \rangle_{\text{FS}}}{(\bar{\lambda}_{\Gamma,j}/4) \omega^2 - \mathbb{M}_{\Gamma,j}^+}. \quad (\text{S96})$$

The resonance of the nematicity mode to the magnetic response is subject to the selection rule due to $\langle \bar{\lambda} (\mathbf{d} \times \mathbf{d}_j^{(\Gamma)})_\nu \rangle_{\text{FS}}$. For the nematicity mode, $\mathcal{D}_{E_u,2}^+$, one finds $\langle [\mathbf{d}_1^{(E_u)} \times \mathbf{d}_2^{(E_u)}]_x \rangle_{\text{FS}} = \langle [\mathbf{d}_1^{(E_u)} \times \mathbf{d}_2^{(E_u)}]_y \rangle_{\text{FS}} = 0$ and $\langle [\mathbf{d}_1^{(E_u)} \times \mathbf{d}_2^{(E_u)}]_z \rangle_{\text{FS}} \neq 0$. This implies the selection rule that the nematicity mode contributes only to the longitudinal dynamical spin susceptibility

$$\chi_{zz}^{\text{CM}} \neq 0, \quad (\text{S97})$$

and otherwise $\chi_{\mu\nu}^{\text{CM}} = 0$. We will study in details the impact of the nematicity mode on dynamical spin susceptibilities elsewhere.

* mizushima@mp.es.osaka-u.ac.jp

- [1] K. Matano, M. Kriener, K. Segawa, Y. Ando, and G.-q. Zheng, *Spin-rotation symmetry breaking in the superconducting state of $\text{Cu}_x\text{Bi}_2\text{Se}_3$* , *Nat. Phys.* **12**, 852 (2016).
- [2] S. Yonezawa, K. Tajiri, S. Nakata, Y. Nagai, Z. Wang, K. Segawa, Y. Ando, and Y. Maeno, *Thermodynamic evidence for nematic superconductivity in $\text{Cu}_x\text{Bi}_2\text{Se}_3$* , *Nat. Phys.* **13**, 123 (2016).
- [3] Y. Pan, A. M. Nikitin, G. K. Araizi, Y. K. Huang, Y. Matsushita, T. Naka, and A. de Visser, *Rotational symmetry breaking in the topological superconductor $\text{Sr}_x\text{Bi}_2\text{Se}_3$ probed by upper-critical field experiments*, *Sci. Rep.* **6**, 28632 (2016).
- [4] A. M. Nikitin, Y. Pan, Y. K. Huang, T. Naka, and A. de Visser, *High-pressure study of the basal-plane anisotropy of the upper critical field of the topological superconductor $\text{Sr}_x\text{Bi}_2\text{Se}_3$* , *Phys. Rev. B* **94**, 144516 (2016).
- [5] T. Asaba, B. J. Lawson, C. Tinsman, L. Chen, P. Corbæ, G. Li, Y. Qiu, Y. S. Hor, L. Fu, and L. Li, *Rotational Symmetry Breaking in a Trigonal Superconductor Nb-doped Bi_2Se_3* , *Phys. Rev. X* **7**, 011009 (2017).
- [6] J. Shen, W.-Y. He, N. F. Q. Yuan, Z. Huang, C.-w. Cho, S. H. Lee, Y. S. Hor, K. T. Law, and R. Lortz, *Nematic topological superconducting phase in Nb-doped Bi_2Se_3* , *npj Quantum Materials* **2**, 59 (2017).
- [7] G. Du, Y. Li, J. Schneeloch, R. D. Zhong, G. Gu, H. Yang, H. Lin, and H.-H. Wen, *Superconductivity with two-fold symmetry in topological superconductor $\text{Sr}_x\text{Bi}_2\text{Se}_3$* , *Sci. China Phys., Mech. & Astron.* **60**, 037411 (2017).
- [8] M. P. Smylie, K. Willa, H. Claus, A. Snezhko, I. Martin, W.-K. Kwok, Y. Qiu, Y. S. Hor, E. Bokari, P. Niraula, A. Kayani, V. Mishra, and U. Welp, *Robust odd-parity superconductivity in the doped topological insulator $\text{Nb}_x\text{Bi}_2\text{Se}_3$* , *Phys. Rev. B* **96**, 115145 (2017).
- [9] M. P. Smylie, K. Willa, H. Claus, A. E. Koshelev, K. W. Song, W.-K. Kwok, Z. Islam, G. D. Gu, J. A. Schneeloch, R. D. Zhong, and U. Welp, *Superconducting and normal-state anisotropy of the doped topological insulator $\text{Sr}_{0.1}\text{Bi}_2\text{Se}_3$* , *Sci. Rep.* **8**, 7666 (2018).
- [10] A. Y. Kuntsevicha, M. Bryzgalova, V. Prudkogliada, V. Martovitskii, Y. Selivanova, and E. Chizhevskii, *Revealing the intrinsic anisotropy of superconducting $\text{Sr}_x\text{Bi}_2\text{Se}_3$* , (2018), [arXiv:1801.09287](https://arxiv.org/abs/1801.09287).

- [11] K. Willa, R. Willa, K. W. Song, G. D. Gu, J. A. Schneeloch, R. Zhong, A. E. Koshelev, W.-K. Kwok, and U. Welp, *Nanocalorimetric Evidence for Nematic Superconductivity in the Doped Topological Insulator $\text{Sr}_{0.1}\text{Bi}_2\text{Se}_3$* , (2018), [arXiv:1807.11136](#).
- [12] L. Fu, *Odd-parity topological superconductor with nematic order: Application to $\text{Cu}_x\text{Bi}_2\text{Se}_3$* , *Phys. Rev. B* **90**, 100509 (2014).
- [13] M. Sato, *Topological odd-parity superconductors*, *Phys. Rev. B* **81**, 220504 (2010).
- [14] L. Fu and E. Berg, *Odd-Parity Topological Superconductors: Theory and Application to $\text{Cu}_x\text{Bi}_2\text{Se}_3$* , *Phys. Rev. Lett.* **105**, 097001 (2010).
- [15] S. Sasaki, M. Kriener, K. Segawa, K. Yada, Y. Tanaka, M. Sato, and Y. Ando, *Topological Superconductivity in $\text{Cu}_x\text{Bi}_2\text{Se}_3$* , *Phys. Rev. Lett.* **107**, 217001 (2011).
- [16] A. Yamakage, K. Yada, M. Sato, and Y. Tanaka, *Theory of tunneling conductance and surface-state transition in superconducting topological insulators*, *Phys. Rev. B* **85**, 180509 (2012).
- [17] L. Hao and T. K. Lee, *Surface spectral function in the superconducting state of a topological insulator*, *Phys. Rev. B* **83**, 134516 (2011).
- [18] T. H. Hsieh and L. Fu, *Majorana Fermions and Exotic Surface Andreev Bound States in Topological Superconductors: Application to $\text{Cu}_x\text{Bi}_2\text{Se}_3$* , *Phys. Rev. Lett.* **108**, 107005 (2012).
- [19] S.-K. Yip, *Models of superconducting $\text{Cu}_x\text{Bi}_2\text{Se}_3$: Single- versus two-band description*, *Phys. Rev. B* **87**, 104505 (2013).
- [20] T. Mizushima, A. Yamakage, M. Sato, and Y. Tanaka, *Dirac-fermion-induced parity mixing in superconducting topological insulators*, *Phys. Rev. B* **90**, 184516 (2014).
- [21] S. Sasaki and T. Mizushima, *Superconducting doped topological materials*, *Physica C* **514**, 206 (2015).
- [22] L. D. Landau and E. M. Lifshitz, *Quantum Mechanics*, Vol. 5 (Pergamon, New York, 1958) Chap. 8.
- [23] P. J. Hirschfeld, P. Wölfle, J. A. Sauls, D. Einzel, and W. O. Putikka, *Electromagnetic absorption in anisotropic superconductors*, *Phys. Rev. B* **40**, 6695 (1989).
- [24] P. J. Hirschfeld, W. O. Putikka, and P. Wölfle, *Electromagnetic power absorption by collective modes in unconventional superconductors*, *Phys. Rev. Lett.* **69**, 1447 (1992).
- [25] S. K. Yip and J. A. Sauls, *Circular dichroism and birefringence in unconventional superconductors*, *J. Low Temp. Phys.* **86**, 257 (1992).
- [26] J. A. Sauls, H. Wu, and S.-B. Chung, *Anisotropy and strong-coupling effects on the collective mode spectrum of chiral superconductors: application to Sr_2RuO_4* , *Front. Phys.* **3**, 36 (2015).
- [27] H. Wu and J. A. Sauls, *Collective mode spectrum and transverse electromagnetic wave response in anisotropic p-wave model for unconventional chiral superconductors*, to be submitted (2018).
- [28] H. Wu, *Excitations in Topological Superfluids and Superconductors*, Ph. D. thesis, Northwestern University (2017).
- [29] R. Roy and C. Kallin, *Collective modes and electromagnetic response of a chiral superconductor*, *Phys. Rev. B* **77**, 174513 (2008).
- [30] S. Higashitani and K. Nagai, *Electromagnetic response of a $k_x \pm ik_y$ superconductor: Effect of order-parameter collective modes*, *Phys. Rev. B* **62**, 3042 (2000).
- [31] M. Miura, S. Higashitani, and K. Nagai, *Effect of Order Parameter Collective Mode on Electronic Raman Spectra of Spin-Triplet Superconductor Sr_2RuO_4* , *J. Phys. Soc. Jpn.* **76**, 034710 (2007).
- [32] D. S. Hirashima, *Dynamical Spin Susceptibilities in the Superconducting Phase of Sr_2RuO_4* , *J. Phys. Soc. Jpn.* **76**, 034701 (2007).
- [33] H. Monien, K. Scharnberg, L. Tewordt, and N. Schopohl, *Effects of spin-orbit interaction and crystal fields on superconducting p-wave pair states and their collective excitations in cubic systems*, *J. Low Temp. Phys.* **65**, 13 (1986).
- [34] D. Fay and L. Tewordt, *Collective order-parameter modes for hypothetical p-wave superconducting states in Sr_2RuO_4* , *Phys. Rev. B* **62**, 4036 (2000).
- [35] S. Maiti and P. J. Hirschfeld, *Collective modes in superconductors with competing s- and d-wave interactions*, *Phys. Rev. B* **92**, 094506 (2015).
- [36] N. Bittner, D. Einzel, L. Klam, and D. Manske, *Leggett Modes and the Anderson-Higgs Mechanism in Superconductors without Inversion Symmetry*, *Phys. Rev. Lett.* **115**, 227002 (2015).
- [37] R. M. Lutchyn, P. Nagornykh, and V. M. Yakovenko, *Gauge-invariant electromagnetic response of a chiral $p_x + ip_y$ superconductor*, *Phys. Rev. B* **77**, 144516 (2008).
- [38] E. Lahoud, E. Maniv, M. S. Petrushevsky, M. Naamneh, A. Ribak, S. Wiedmann, L. Petaccia, Z. Salman, K. B. Chashka, Y. Dagan, and A. Kanigel, *Evolution of the Fermi surface of a doped topological insulator with carrier concentration*, *Phys. Rev. B* **88**, 195107 (2013).
- [39] B. J. Lawson, G. Li, F. Yu, T. Asaba, C. Tinsman, T. Gao, W. Wang, Y. S. Hor, and L. Li, *Quantum oscillations in $\text{Cu}_x\text{Bi}_2\text{Se}_3$ in high magnetic fields*, *Phys. Rev. B* **90**, 195141 (2014).
- [40] H. Zhang, X.-L. Qi, X. Dai, Z. Fang, and S.-C. Zhang, *Topological insulators in Bi_2Se_3 , Bi_2Te_3 and Sb_2Te_3 with a single Dirac cone on the surface*, *Nat. Phys.* **5**, 438 (2009).
- [41] C.-X. Liu, X.-L. Qi, H. Zhang, X. Dai, Z. Fang, and S.-C. Zhang, *Model Hamiltonian for topological insulators*, *Phys. Rev. B* **82**, 045122 (2010).
- [42] T. Hashimoto, K. Yada, A. Yamakage, M. Sato, and Y. Tanaka, *Bulk Electronic State of Superconducting Topological Insulator*, *J. Phys. Soc. Jpn.* **82**, 044704 (2013).
- [43] L. Hao, G.-L. Wang, T.-K. Lee, J. Wang, W.-F. Tsai, and Y.-H. Yang, *Anisotropic spin-singlet pairings in $\text{Cu}_x\text{Bi}_2\text{Se}_3$ and Bi_2Te_3* , *Phys. Rev. B* **89**, 214505 (2014).
- [44] See Supplemental Material [url] for quasiclassical Keldysh theory and time-dependent Ginzburg-Landau theory, which includes Refs. [61].
- [45] J. W. F. Venderbos, V. Kozii, and L. Fu, *Odd-parity superconductors with two-component order parameters: Nematic and chiral, full gap, and Majorana node*, *Phys. Rev. B* **94**, 180504 (2016).
- [46] T. Hashimoto, K. Yada, A. Yamakage, M. Sato, and Y. Tanaka, *Effect of Fermi surface evolution on superconducting gap in superconducting topological insulator*, *Supercond. Sci. Technol.* **27**, 104002 (2014).
- [47] N. F. Q. Yuan, W.-Y. He, and K. T. Law, *Superconductivity-induced ferromagnetism and Weyl superconductivity in Nb-doped Bi_2Se_3* , *Phys. Rev. B* **95**, 201109 (2017).
- [48] L. Chirrolli, F. de Juan, and F. Guinea, *Time-reversal and rotation symmetry breaking superconductivity in Dirac materials*, *Phys. Rev. B* **95**, 201110 (2017).
- [49] A. A. Zyuzin, J. Garaud, and E. Babaev, *Nematic Skyrmions in Odd-Parity Superconductors*, *Phys. Rev. Lett.* **119**, 167001 (2017).
- [50] L. Chirrolli, *Chiral superconductivity in thin films of doped Bi_2Se_3* , *Phys. Rev. B* **98**, 014505 (2018).
- [51] P. W. Anderson, *Plasmons, Gauge Invariance, and Mass*, *Phys. Rev.* **130**, 439 (1963).
- [52] P. W. Higgs, *Broken Symmetries and the Masses of Gauge Bosons*, *Phys. Rev. Lett.* **13**, 508 (1964).
- [53] J. Serene and D. Rainer, *The quasiclassical approach to superfluid ^3He* , *Phys. Rep.* **101**, 221 (1983).
- [54] G. Eilenberger, *Transformation of Gorkov's equation for type II superconductors into transport-like equations*, *Z. Phys.* **214**, 195 (1968).

- [55] J. A. Sauls and T. Mizushima, *On the Nambu fermion-boson relations for superfluid ^3He* , *Phys. Rev. B* **95**, 094515 (2017).
- [56] T. Tsuneto, *Transverse Collective Excitations in Superconductors and Electromagnetic Absorption*, *Phys. Rev.* **118**, 1029 (1960).
- [57] R. H. McKenzie and J. A. Sauls, *Collective Modes and Nonlinear Acoustics in Superfluid $^3\text{He-B}$* , in *Helium Three*, edited by W. P. Halperin and L. P. Pitaevskii (Elsevier, Amsterdam, 1990) p. 255, [arXiv:1309.6018](#).
- [58] K. Machida, *Spin Triplet Nematic Pairing Symmetry and Superconducting Double Transition in $\text{U}_{1-x}\text{Th}_x\text{Be}_{13}$* , *J. Phys. Soc. Jpn.* **87**, 033703 (2018).
- [59] L. Andersen, Z. Wang, T. Lorenz, and Y. Ando, *Nematic superconductivity in $\text{Cu}_{1.5}(\text{PbSe})_5(\text{Bi}_2\text{Se}_3)_6$* , *Phys. Rev. B* **98**, 220512 (2018).
- [60] K. A. M. Hasan Siddiquee, R. Munir, C. Dissanayake, P. Vaidya, C. Nickle, E. Del Barco, D. VanGennep, J. Hamlin, and Y. Nakajima, *Nematic superconductivity in topological semimetal CaSn_3* , (2019), [arXiv:1901.02087](#).
- [61] D. Rainer and J. A. Sauls, *Strong-Coupling Theory of Superconductivity*, in *Superconductivity: From Basic Physics to New Developments*, edited by P. N. Butcher and Y. Lu (World Scientific, Singapore, 1995) pp. 45–78, http://dx.doi.org/10.1142/9789814503891_0002, [arXiv:1809.05264](#).
- [62] T. Mizushima and J. A. Sauls, *Bosonic Surface States and Acoustic Spectroscopy of Confined Superfluid $^3\text{He-B}$* , (2018), [arXiv:1801.02277](#).
- [63] A. Vorontsov and J. A. Sauls, *Thermodynamic Properties of Thin Films of Superfluid $^3\text{He-A}$* , *Phys. Rev. B* **68**, 064508 (2003).